INSTITUTO DE QUÍMICA
PROGRAMA DE PÓS GRADUAÇÃO EM GEOCIÊNCIAS – GEOQUÍMICA

DANIEL FRANÇOIS DO NASCIMENTO SILVA

FORAMINIFERAL ASSEMBLAGES AND TEST CHARACTERISTICS ASSOCIATED WITH NATURAL LOW PH WATERS AT PUERTO MORELOS REEF LAGOON SPRINGS, QR MEXICO

NITERÓI
2022

DANIEL FRANÇOIS DO NASCIMENTO SILVA

FORAMINIFERAL ASSEMBLAGES AND TEST CHARACTERISTICS ASSOCIATED WITH NATURAL LOW PH WATERS AT PUERTO MORELOS REEF LAGOON SPRINGS, QR MEXICO

Dissertation presented to the Pos Graduation Program in Geosciences of the Universidade Federal Fluminense in Partial Fulfillment of the Requirements for the Degree of Master of Science.Area of Concentration: Environmental Geochemistry.

Supervisor

Prof. Dr. Cátia Fernandes Barbosa

Co-supervisor:

Prof. Dr. Adina Paytan

NITERÓI

2022

Ficha catalográfica automática - SDC/BGQ
Gerada com informações fornecidas pelo autor

S586f Silva, Daniel Francois do Nascimento
Foraminiferal assemblages and test characteristics associated with natural low pH waters at Puerto Morelos reef lagoon springs, QR Mexico / Daniel Francois do Nascimento Silva. - 2022.
59 f.: il.

Orientador: Cátia Fernandes Barbosa.
Coorientador: Adina Paytan.
Dissertação (mestrado)-Universidade Federal Fluminense, Instituto de Química, Niterói, 2022.

1. Foraminífero bentônico. 2. Acidificação. 3. Mudança climática. 4. Ecologia. 5. Produção intelectual. I. Barbosa, Cátia Fernandes, orientadora. II. Paytan, Adina, coorientadora. III. Universidade Federal Fluminense. Instituto de Química. IV. Título.

CDD - XXX

Bibliotecário responsável: Debora do Nascimento - CRB7/6368

DANIEL FRANÇOIS DO NASCIMENTO SILVA

Foraminiferal assemblages and test characteristics associated with natural low pH waters at Puerto Morelos reef lagoon springs, QR Mexico

Dissertation presented to the Pos Graduation Program in Geosciences of the Universidade Federal Fluminense in Partial Fulfillment of the Requirements for the Degree of Master of Science.Area of Concentration: Environmental Geochemistry.

COMMITTEE MEMBERS

_____

Cátia Fernandes Barbosa, Committee Chair (Universidade Federal Fluminense)

_____

Adina Paytan, Committee Member (University of California – Santa Cruz, USA)

_____

Prof. Dr. Heitor Evangelista da Silva, Committee Member (Universidade do Estado do Rio de Janeiro)

_____

Prof. Dr. Pamela Hallock Muller, Committee Member (University of South Florida, USA)

NITERÓI

2022

ACKNOWLEDGMENTS

Firstly, I must thank my advisor and friend, Cátia Fernandes Barbosa, for teaching me avidly over the last 5 years. Cátia thanks to you I was introduced to this microworld and trained to be a micropaleontologist. I also thank my co-supervisor Adina Paytan for giving me the great opportunity to work on such an important topic as acidification and its effects on marine organisms. Over the last 2 years, we have all been working remotely together through a difficult time, but I have learned a lot from the two of you, and I am sincerely grateful for that. Your guidance broadened my perspectives and made my master's degree more memorable.

To Elisabeth Crook for the help with the environmental data and Dr. Olga and Ricardo for the partnership and collaboration with the microtomography analyses. I also thank to my friend Luiza Reis which helped me with the statistics performed in this study.

To my committee members Pamela Hallock and Heitor Evangelista for their great contributions to this dissertation.

To my friends Nayara Dornelas, Lara Juno, Victoria Perfeito, Joyce Bozi, Camila Areias, Grazielle Nascimento, Matheus Vianna and Suzan Costa for their psychological support and for believing in me.

To my family and my boyfriend Filipe who have accompanied me during all these years.

To the CNPQ for the scholarship (process No. 132210/2020-7) I received during the masters and for supporting Brazilian science.

ABSTRACT

Ocean acidification is expected to negatively affect many ecologically important organisms. Here we explored the response of Caribbean benthic foraminiferal assemblages to naturally discharging low-pH waters similar to expected future projections for the end of the 21st century. At low pH (~7.7 pH units) and low calcite saturation, agglutinated and symbiont-bearing species were relatively more abundant, indicating higher resistance to potential carbonate chemistry changes. Diversity and other taxonomical metrics declined steeply with decreasing pH, despite exposure of this ecosystem for millennia to low pH conditions, suggesting that tropical foraminifera communities will be negatively impacted under acidification scenarios SSP3-7.0 and SSP5-8.5. The species *Archaias angulatus*, a major contributor to sediment production in the Caribbean, was able to calcify at conditions more extreme than those projected for the late 21st century (7.1 pH units), but the calcified tests were of lower density than those exposed to higher-pH ambient conditions (7.96 pH units), indicating that reef foraminiferal carbonate budget might decrease. Smaller foraminifera were highly sensitive to decreasing pH and our results demonstrate their potential as indicators to monitor increasing OA conditions.

Keywords: benthic foraminifera; ocean acidification; taphonomy; assemblage; epibenthic ecology; CMIP6.

RESUMO

Espera-se que a acidificação dos oceanos (AO) afete negativamente muitos organismos ecologicamente importantes. No presente trabalho foi explorado o potencial de aclimatação de assembleias caribenhas de foraminíferos bentônicos associados a nascentes de baixo pH que simulam realisticamente projeções futuras para o final do século. Em condições de baixo pH (7.7 unidades de pH), foraminíferos aglutinantes e com endossimbiontes foram relativamente mais resistentes, respondendo positivamente às mudanças na química do carbonato. No entanto, a diversidade e outras métricas taxonômicas da comunidade diminuíram acentuadamente com a diminuição do pH, apesar de sua exposição geracional a essas condições, sugerindo que os foraminíferos serão negativamente afetados nos cenários SSP3-7.0 e SSP5-8.5. A espécie *Archaias angulatus*, um dos principais contribuintes para a produção de sedimentos no Caribe, foi capaz de calcificar em condições ácidas (7,1 unidades de pH) muito além das previstas para o final do século, mas os testas calcificadas em baixo pH apresentaram uma menor densidade do que os grupos que viviam em condições controle (7,96 unidades de pH), indicando que o balanço da produção carbonática de foraminíferos recifais pode diminuir. Além disso, foraminíferos menores foram altamente sensíveis à diminuição do pH e nossos resultados demonstram seu potencial para monitorar o aumento da OA.

Palavras-chave: foraminíferos bentônicos; acidificação dos oceanos; tafonomia; assembleia; ecologia epibentônica.

LIST OF FIGURES

LIST OF TABLES

LIST OF ABREVIATIONS

A_T	Total Alkalinity
CCA	Canonical Correspondence Analysis
CMIP6	Couple Model Intercomparison Project Phase Six
C_T	Total inorganic Carbon
RCPs	Representative Concentration Pathways
H'	Shannon-Weiner Diversity
ID	Identification
IPCC	Intergovernmental Panel on Climate Change
J	Pielou's evenness
LBF	Large Benthic Foraminifera
M	Meters
nMDS	non-Metric Multidimensional Scaling
OA	Ocean Acidification
PM	Puerto Morelos
S	Species richness
SIMPER	SIMilarity PERcentages analysis
SSPs	Shared Socioeconomic Pathways
T	Temperature
Ω	Saturation-state
Ω-Calcite	Calcite saturation state

TABLE OF CONTENT

1 INTRODUCTION

With anthropogenic carbon emissions steadily increasing since the beginning of the industrial age, atmospheric carbon dioxide (CO_2) is now higher than pre-industrial values (PETIT *et al.*, 1999; LÜTHI *et al.*, 2008). Global emissions driven primarily by fossil fuel burning and land-use change increased atmospheric CO_2 concentrations from approximately 277 parts per million (ppm) in 1750 to 415 ppm at present, an increase of roughly 2 ppm/yr (LE QUÉRÉ *et al.*, 2018; LICKER *et al.*, 2019). This increase in atmospheric CO_2 resulted in a proportional oceanic CO_2 uptake (~118Pg C, SABINE *et al.*, 2004), and decrease of surface ocean pH, a process referred as "ocean acidification" (DONEY *et al.*, 2009). During this process the absorbed CO_2 reacts with water to form carbonic acid,

$$CO_2 + H_2O \leftrightarrow H_2CO_3^-$$

which further dissociates into bicarbonate ions by releasing hydrogen ions (H^+):

$$CO_2 + H_2O \leftrightarrow HCO_3^- + H^+$$

The released H^+ further reacts with carbonate to form more bicarbonate,

$$CO_3^{2-} + H^+ + H_2O \leftrightarrow 2HCO_3^-$$

which results in decreased carbonate ion concentrations and, therefore, carbonate saturation state (Ω), defined as

$$\Omega = \frac{[CO_3^{2-}][Ca^{2+}]}{K_{sp}}$$

where K'sp is the solubility product (e.g., of calcite or aragonite) that depends on other abiotic parameters like temperature, salinity, and pressure (DONEY *et al.*, 2020).

Seawater pH levels have already decreased on average by 0.1 units and future projections suggests a further acidification by the end of the 21st century (KWIATKOWSKI *et al.*, 2020; INTERGOVERNMENTAL PANEL ON CLIMATE CHANGE, 2021). These projections, if materialized, are expected to have serious implications to many calcifying organisms that require seawater carbonate saturation state $\Omega > 1$ for calcification, especially those that deposit more soluble $CaCO_3$ mineral phases such as aragonite and high-Mg calcite.

Foraminifera, widely abundant members of benthic communities, are of particular interest due to their important role in global biochemical cycles. Often ignored for their small size, they are vital contributors to $CaCO_3$ cycling (LANGER *et al.*, 1997; LANGER, 2008;), and relevant for organic carbon cycling in many ecosystems (MOODLEY *et al.*, 2000). Once dead, their tests also become important contributors to sediment accumulation (DOO *et al.*, 2016; YAMANO; MIYAJIMA; KOIKE, 2000) and are an important component of the long-term carbon burial flux in the ocean (SCHIEBEL, 2002). Previous research has demonstrated

that, in general, lower pH conditions are associated to reduced calcification (SINUTOK *et al.*, 2014; GUAMÁN-GUEVARA *et al.*, 2019), and community shifts from calcareous to agglutinated-dominated assemblages (DIAS *et al.*, 2010; PETTIT *et al.*, 2015; MARTINEZ *et al.*, 2018; WEINMANN *et al.*, 2021). However, some studies have also demonstrated either resilience (ENGEL *et al.*, 2015; PETTIT *et al.*, 2015; STUHR *et al.*, 2021), or even positive effects on foraminifera, such as enhanced calcification (FUJITA *et al.*, 2011) and enzymatic calcification activity (PRAZERES *et al.*, 2015), which demonstrate the complexity of interspecific responses to OA.

To better understand future impacts of OA on foraminifera this dissertation aimed to evaluate foraminiferal responses and community changes for projected emissions scenarios to the end of 21st century (KWIATKOWSKI *et al.*, 2020; INTERGOVERNMENTAL PANEL ON CLIMATE CHANGE, 2021). Specifically, we used the Shared Socioeconomic Pathways (SSPs) framework that provides five distinct scenarios of future socioeconomic developments and respective challenges for mitigation and adaptation to climate change. They were designed along the sixth phase of the Climate Model Intercomparison Project (CMIP6) to be used in the sixth assessment report of the Intergovernmental Panel on Climate Change (IPCC) in combination with the Representative Concentration Pathways (RCPs) (RIAHI *et al.*, 2017). The SSP's (reviewed in RIAHI *et al.*, 2017) include the following scenarios: a world of sustainability that respects environmental boundaries (SSP1-2.6); a "middle of the road" world where trends follow historical patterns (SSP2-4.5); a world of resurgent nationalism and regional conflicts (SSP3-7.0); a world of ever-increasing inequality (SSP4); and a world of unconstrained growth based on the exploitation of abundant fossil fuel resources (SSP5-8.5). The projections are in the range of −0.16 for SSP1-2.6 to −0.44 for SSP5-8.5, from the most conservative to the highest acidification scenario (KWIATKOWSKI *et al.*, 2020; INTERGOVERNMENTAL PANEL ON CLIMATE CHANGE, 2021).

In chapter three "acidification impacts and acclimation potential of foraminifera" are explored in the above explained projection baselines the responses of in situ foraminifera communities living in association with low-pH waters discharged at six submarine groundwater springs in the Caribbean coast of Mexico. By discharging low-pH waters for millennia (BACK *et al.*, 1979), these sites were used to study foraminiferal multi-generational acclimation potential relevant for realistically assessing future projections for the end of the 21st century (ANDERSSON *et al.*, 2015). The chapter comprises a submitted manuscript, replacing the classic dissertation structure. The conclusions are present in chapter four with the following supplementary materials.

2 OBJECTIVES

2.1 Overarching objective

To evaluate foraminiferal responses and community changes to projected acidification scenarios for the end of 21st century considering all Shared Socioeconomic Pathways (SSPs) described at the Coupled Model Intercomparison Project Phase Six (CMIP6) and explore possible acclimation patterns in foraminiferal species. Additionally, we aim to explore *postmortem* alterations for a better understanding and interpretation of potential changes to carbonate deposition.

2.2 Specific objectives

- To analyze foraminiferal assemblage structure trends along a gradient of changing pH, assessing changes in the taxonomic metrics, including abundance (N), Species richness (S), Shannon-Wiener diversity (H′), Pielou's evenness (J′), and assemblage composition.
- To quantify the extent to which foraminiferal tests along the above gradient have been taphonomically altered based on larger-scale structural damage such as widespread corrosion and breakage.
- To explore changes in the size of specimens making up the assemblage by quantifying the surface area of all individuals picked using the ImageJ software.
- To employ an X-ray MicroCT scanning analysis to evaluate possible acclimation patterns in the shell structure of the species *Ar. angulatus* based on changes in density and chamber wall thickness.

3 ACIDIFICATION IMPACTS AND ACCLIMATION POTENTIAL OF FORAMINIFERA

With anthropogenic carbon emissions steadily increasing since the beginning of the industrial age, atmospheric carbon dioxide (CO_2) is now higher than it has been in the past 800,000 years (PETIT *et al.*, 1999; LÜTHI *et al.*, 2008). Global emissions are annually increasing (~2 ppm/yr, LE QUÉRÉ *et al.*, 2018) and leading a proportional increase of CO_2 uptake by the oceans and consequently decrease of surface ocean pH (-0.0181 ± 0.0001 decade^{-1}, LIDA *et al.*, 2020) and carbonate ion concentrations [CO_3^{2-}], a process known as ocean acidification (OA) (DONEY *et al.*, 2020). Following the results of the Coupled Model Intercomparison Project Phase Six (CMIP6), a further decrease of surface ocean pH is expected for all Shared Socioeconomic Pathways (SSPs) at the end of the 21st century (KWIATKOWSKI *et al.*, 2020; INTERGOVERNMENTAL PANEL ON CLIMATE CHANGE, 2021). As the carbonate system has major control on biogenic calcification efficiency, this process is expected to negatively affect many ecologically important calcifying organisms such as corals (KROEKER *et al.*, 2013; HUGHES *et al.*, 2017), foraminifers (UTHICKE; MOMIGLIANO; FABRICIUS, 2013; KAWAHATA *et al.*, 2019), and coralline crustose algae (PENÃ *et al.*, 2021).

Among these, foraminifera are dominant members of benthic communities with widespread distribution in the oceans. During their lifespan, they are vital to $CaCO_3$ cycling, especially through calcification (LANGER *et al.*, 1997; LANGER, 2008). On a global scale, they are estimated to contribute a total of 14 billion tons of calcium carbonate per year, which accounts for about 25% of current total calcium carbonate production (LANGER, 2008). Due to their ability to consume substantial amounts of organic matter, they are also relevant for organic carbon cycling (MOODLEY *et al.*, 2000), being part of a key link in marine food chains. After death, their tests became important contributors to sediment mass accumulation in many ecosystems (YAMANO; MIYAJIMA; KOIKE, 2000; DOO *et al.* 2016) and are also relevant for the carbon burial flux in the ocean (SCHIEBEL, 2002). With ongoing OA and future scenarios projecting rapid changes (KWIATKOWSKI *et al.*, 2020; INTERGOVERNMENTAL PANEL ON CLIMATE CHANGE, 2021), it is vital to understand how foraminifera will be affected for assessing biological feedbacks and changes in biochemical cycles. To date, many studies under controlled conditions often document the association of low-pH with decreased calcification, weight, size, and taxonomical metrics (NEHRKE *et al.*, 2013; KAWAHATA *et al.*, 2019; NARAYAN *et al.*, 2021, and references

therein). However, relatively little is known about how foraminifera respond in natural low-pH low carbonate saturation waters, which is crucial for determining if and how communities have the potential to acclimate.

In situ investigations have been performed in natural CO_2 vents in the Mediterranean Sea (DIAS *et al.*, 2010; PETTIT *et al.*, 2015), Papua New Guinea (UTHICKE; MOMIGLIANO; FABRICIUS, 2013), the northern Gulf of California (PETTIT *et al.*, 2013) and coastal springs in Puerto Morelos (PM), Mexico (MARTINEZ *et al.*, 2018). In the latter, recruitment and early succession (CROOK *et al.*, 2016), acclimatization potential (CROOK *et al.*, 2013), and the responses of calcifying assemblages were studied (CROOK *et al.*, 2012; MARTINEZ *et al.*, 2018), notably demonstrating that, despite general deleterious effects, some calcifiers were relatively resilient to OA. Specifically, a study focused on Large Benthic Foraminifera (LBF) has shown that porcelaneous, chlorophyte-bearing foraminifera, (e.g., *Archaias angulatus*), were relatively less impacted (MARTINEZ *et al.*, 2018). Study sites such as coastal springs allow the investigation of foraminiferal communities under projected future conditions more realistically, helping to decrease the uncertainty in global-scale models. However, a detailed survey considering community-wide responses (i.e., including smaller foraminifera) is necessary to ascertain a wider range of potential impacts.

As CO_2 emissions continue to grow despite emerging climate policies (PETERS *et al.*, 2020), global awareness has demonstrated a strong interest in research focused on potential impacts for mitigative action. To build on and expand the findings at PM we aimed to (i) investigate the effects of OA on both large and small foraminiferal assemblages for acidification scenarios projected to the end of 21st century (KWIATKOWSKI *et al.*, 2020; INTERGOVERNMENTAL PANEL ON CLIMATE CHANGE, 2021), (ii) explore the taphonomical and ecological implications of *postmortem* alterations for reef ecosystems, and (iii) investigate possible acclimation patterns in the shell structure of the species *Ar. angulatus*. Specifically, an examination of assemblage structure, taxonomic metrics, assemblage test size, preservation potential, and an X-ray micro-CT analysis in the species *Ar. angulatus* was employed.

3.1 Methods

3.1.1 Study site and data retrieval

The Yucatán Peninsula is a karstic region in Southern Mexico (Fig. 1A). The geology is dominated by Tertiary limestones underlain by an ejecta/evaporite complex, where

several structural and tectonic features strongly influence and divide the area into six distinct physiographic regions (BACK; HANSHAW, 1970). Among these, Puerto Morelos reef lagoon is part of the Holbox Fracture Zone–Xel-Ha region, which is characterized by >100 km long chain of elongated depressions referred as 'sabanas' (PERRY; VELAZQUEZ-OLIMAN; MARIN, 2002). In this area, rainwater infiltrates the porous karstic limestone of Quintana Roo (Fig. 1B) and flows towards the ocean through interconnected caves and fractures where the groundwater mixes with seawater in the underground aquifers before discharging between the shore and the offshore barrier reef (BEDDOWS *et al.*, 2007; NULL *et al.*, 2014). Flowing through the limestones and interacting with the strata through processes of dissolution, precipitation, and mixing, the groundwater conditions change and finally discharge along the Mexican coast as low-pH, low carbonate-saturation-state (Ω), and high inorganic C content waters (BACK; HANSHAW, 1970; PERRY *et al.*, 2002; CROOK *et al.*, 2012, 2013, 2016; MARTINEZ *et al.*, 2018, 2019). These waters discharge at submarine springs, which structure ranges from long ''fractures'' to small circular depressions "seeps" (Fig. 1D, spring Agua), (CROOK *et al.*, 2012). The discharge of the springs is relatively constant throughout the year, and lower salinity and pH levels are recognized to occur only during low tide in the rainy season for no more than a one hour (CROOK *et al.*, 2016).

Surface sediment samples (~1 cm depth, coarse sand) were retrieved using a spoon at various distances from the center of six submarine springs (Fig.1C, Gorgos, Laja, Mini, Norte, Agua, and Pargos) in October 2011. In the laboratory, samples were weighed, washed with deionized water through a 63 µm sieve mesh, and dried at 50°C for 24 hours. Discrete water samples near the site of sediment collection were also retrieved for water chemical analysis. Water samples were filtered (0.2 µm filter) and split into aliquots for the analysis of Water samples were filtered (0.2 µm) and split into aliquots for the analysis of salinity, total inorganic carbon (C_T) and total alkalinity (A_T), following the protocols of Dickson, Sabine and Christian (2007). The C_T was measured on a CM5011 Carbon Coulometer (UIC, Inc.; analytical measurement error: ± 3 µmol kg−1) and T_A using an automated open-cell, potentiometric titrator (Orion model 950; analytical measurement error: ±2 µmol kg−1). Salinity was measured using a portable salinometer (Portasal Model 8410, Guild Line). Seawater temperature was measured in situ with a handheld YSI analyzer (Yellow Springs model 63). Water pH, carbonate ion concentration (CO_3^{2-}) and calcite saturation state (Ω-Calcite) were calculated using the program CO_2Sys (PIERROT; LEVIS; WALLACE, 2006), considering the CO_2 dissociation constants of Lueker, Dickson and Keeling (2000); $KHSO_4$ – Dickson, Sabine and Christian (2007); B concentration – UPPSTRÖM, 1974. Certified CO_2

reference material (from A. Dickson lab at UC San Diego, batch 112) was used to calibrate all instruments.

Figure 1 – (A) Location map of the Yucatán Peninsula, (B) Quintana Roo, and (C) the six submarine springs (Gorgos, Laja, Mini, Norte, Pargos and Agua) studied at Puerto Morelos reef Lagoon (National Marine Park)

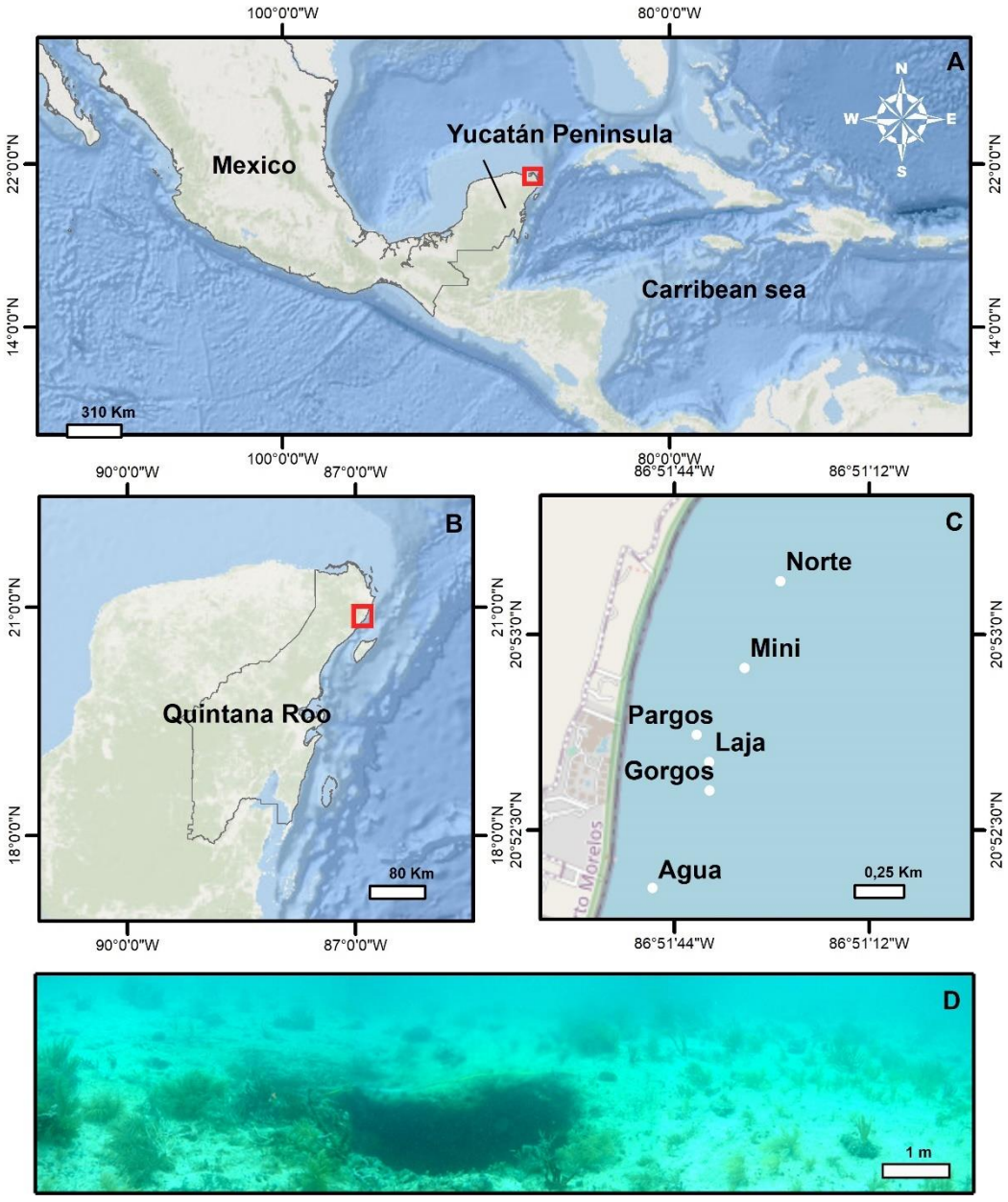

Source: PRODUCED BY THE AUTHOR, 2022

3.1.2 Foraminiferal analysis

The dry weight of sediments was recorded, and samples were split to make them more suitable and efficient to pick. The specimens found in each pre weighed sediment aliquot were counted under a Zeiss STEMI 2000 stereomicroscope until a minimum of 250 specimens were obtained from each sample. Foraminiferal tests were identified to the lowest possible taxonomic level and assigned to informal species categories for diversity analyses.

The taxonomic classification was based on the specialized bibliography of Cushman (1929), Jones (1994), and supplementary taxonomic studies (MILKER; SCHMIEDL, 2012; ABU-ZIED; AL-DUBAI; BANTAN, 2016; SARIASLAN; LANGER, 2021). Each species and genus were verified against WoRMS to ensure the use of the most recent nomenclature.

The samples were stained in rose Bengal to consider the living counts in faunal analysis. Specimens were considered “alive” when all chambers, except for the last one or two, were well stained. Non-transparent agglutinated and miliolid taxa were broken to inspect their contents. Proportions of stained specimens were small (~3%) and hence total (live plus dead) assemblages were used. The low live percentage is a common pattern as most reef-dwelling taxa tend to live on phytal or hard substrates rather than directly on the sediments (MARTIN, 1986; BARBOSA *et al.*, 2009, 2012; STEPHENSON; HALLOCK; KELMO, 2015). Shannon-Weiner Diversity Index (H′), and Pielou’s evenness (J′) were calculated considering the standardized foraminiferal density at 1 ml. These taxonomic metrics were calculated as follows: Shannon-Weiner Diversity Index with the equation $H' = -\Sigma(Pi * \log(Pi))$, where Pi is the proportion of individuals per species; Pielou's evenness with the equation $J' = H'/\log(S)$, where H′ is the Shannon-Weiner Diversity Index and S the species richness. Assemblage distributions were also assessed according to differences in functional groups, i.e., symbiont-bearing and opportunistic, and test type groups, i.e., small miliolids, small rotaliids, and agglutinated that do not present an opportunistic behavior. This approach is used by Amergian *et al.* (2022), based on categories designed by Hallock *et al*. (2003) for sensitivity/stress-tolerance taxa and Murray (2006) for different test compositions.

3.1.3 Taphonomy and assemblage test-size analysis

To improve the understanding of the extent to which tests have been taphonomically altered, a quantitative taphonomical analysis was conducted using a light microscope considering larger-scale structural damage such as breakage and dissolution. In the latter, any sign of dissolution, even if minimal, was considered. For a complete survey of the assemblage test-size distribution the surface area of all individuals was calculated using the ImageJ software (SCHNEIDER; RASBAND; ELICEIRI, 2012). All specimens picked were placed on the dorsal side in common brass picking trays and photographed under the same magnification and camera settings using an adapter for a microscope camera. A similar procedure was performed by Prazeres *et al.* (2015) to trace surface area changes (i.e., gain or loss) in large benthic foraminiferal species under low-pH conditions. The parameter of surface area was the most suitable for the analysis since it identifies the size of the foraminiferal tests

in a standard way, considering the high taxonomical and consequently morphological diversity of PM samples.

3.1.4 X-ray MicroCT

An X-ray MicroCT analysis was employed in four individuals from high (7.96 pH units) and low-pH conditions (7.11 pH units). To ensure that the analyzed tests represent living conditions, only tests in excellent condition, and therefore, not influenced by post-mortem processes of dissolution and transport were selected. For the X-ray microCT acquisition, a V/TOMEX/M (GE Measurement & Control Solutions, Wunstorf, Germany) was used. The microCT parameters for the acquisition included a voltage of 60 kV, an energy of 100 μA, 5 frames, and an Al filter with a thickness of 0.5 mm. The geometry had a magnification of 31.81, pixel size of 6.28 μm. Certified calcite standards were used to calibrate the density for this material. The 3D reconstructions were performed using the Phoenix Datos X Reconstruction software, in which the slice alignment, beam hardening correction were implemented, and a mathematical edge-enhancement filter was applied to achieve a higher contrast between the edges. For the 3D visualization, VG Studio Max v 3.0 and Avizo 2020.3 software was used. For calcite density analysis, the CTAnalyser v. 1.18.4.0 software was used. Calcite density was assessed by the calcite density distribution calculated from the CT number that was calculated based on the X-ray attenuation coefficient of each sample. In addition, the estimation of morphometric parameters such as total volume and chamber wall thickness distribution was performed.

3.1.5 Statistical analysis

Cluster analysis of group average was performed using a similarity matrix (Bray-Curtis) of square-root-transformed abundances of foraminifera (≥3%) with a second permutation procedure, the similarity profile (SIMPROF) routine (CLARKE; GORLEY, 2006). The matrix was also used to perform the similarity percentages analysis (SIMPER) to define which species contributed most to the forming groups considering a 90% cut. Non-metric multidimensional scaling (nMDS) was used to visualize the similarity in foraminiferal assemblages. A BIO-ENV procedure (9999 permutations) and global BEST test (statistical significance) was used to identify the set of explanatory environmental parameters that produced a Euclidean matrix that best correlated (Spearman method) the species assemblage similarity matrix and normalized environmental variables. A Canonical Correspondence Analysis (CCA) was also used to explore the relationship between the biological and water

chemistry data. Data normality and variance homogeneity were tested using Shapiro-Wilk and Levene's Test. For comparison of *Ar. angulatus* microstructure parameters between high and low-pH the student's t-test was used for variables with normal distributions and homogenous variances. When these conditions were not met, Welch's t-test was performed. We used the Kruskall-Wallis test to assess differences between functional groups, taxonomic metrics, and assemblage test size. The stations were separated into four groups considering the following pH gradients in respect to future projections: 8.1–8.05 pH units as present-day conditions; 8–7.9 pH units surveying low-intermediate acidification scenarios SSP1-2.6 and SSP2-4.5; 7.8–7.7 surveying high acidification scenarios SSP3-7.0 and SSP5-8.5; 7.6–7.2 surveying acidification conditions beyond those predicted to the end of 21st century. SIMPER, SIMPROF, nMDS, and BIO-ENV procedure were performed in Primer v.6 software (CLARKE; GORLEY, 2006). Student's t-test, Welch's t-test, Kruskal-Wallis tes and data visualization were performed using R software (version 4.0.2; http://www.Rproject.org, R CORE TEAM, 2020). The CCA analysis was perform in PAlaeontological STatistics-PAST software (version 4.09).

3.2 Results

3.2.1 Water chemistry

Seawater carbonate chemistry (Table 1) contrasted strongly between samples. Obtained ranges were as follows: pH = 7.2–8.1 units, Ω-Calcite = 1.3–6.2, CO_3^{2-} = 52–240 µmol/kg^{-1}, T_A = 2044–3108 µmol/kg^{-1}, and C_T = 1725–3197 µmol/kg^{-1}. The temperature was consistent in ranging from 26.1–27.9 while salinity decreased with proximity to the springs, ranging from 28–37. As described in previous studies conducted at the same sites, the salinity at the springs is > 30 over 90% of the time and does not drop below 27 (CROOK *et al.*, 2012), and therefore is expected to produce little to no effect on foraminiferal communities (MARTINEZ *et al.*, 2018). The BIOENV analysis and global BEST test revealed that the best combination (p-value = 0.01) of environmental variables with species abundance was observed when considering pH, CO_3^{2-}, Ω Calcite and T (ρ = 0.55), in which CO_3^{2-} and pH were the environmental variables matching the highest correlation (ρ = 0.5) and temperature the lowest (ρ = 0.038).

Table 1 – Carbonate chemistry parameters of discrete water samples collected near the substrate at the time of sediment collection. T_A = total alkalinity; C_T = total inorganic carbon; CO_3^{2-} = carbonate ion concentration; Ω Calcite = calcite saturation-state; T = temperature

Site	Depth (m)	Sample ID	A_T (µmol/kg^{-1})	C_T (µmol/kg^{-1})	pH	CO_3^{2-} µmol/kg^{-1})	Ω Calcite	T (C°)	Salinity
Norte	5.8	1	2611	2588	7.38	67.03	1.66	27.5	32.21
		2	2734	2734	7.34	60.93	1.53	27.2	30.70
		3	2699	2694	7.34	62.20	1.54	27.2	31.90
		4	2451	2314	7.66	118.47	2.85	27.0	35.25
Pargos	6.8	6	3000	3048	7.23	52.73	1.33	27.6	29.95
		7	3054	3047	7.38	71.16	1.82	27.7	28.00
		8	2304	2160	7.72	119.78	2.97	27.6	32.00
		9	2387	2084	8.00	220.39	5.36	27.5	34.20
		10	2336	2012	8.01	229.56	5.49	27.6	36.17
Gorgos	7.2	12	2350	2065	7.98	207.09	5.03	27.3	34.40
		13	2364	2004	8.10	255.79	6.18	26.8	34.80
		14	2044	1725	8.09	21608	5.24	26.9	34.40
		15	2325	2033	7.96	209.44	5.02	27.8	35.90
Laja	5.8	16	2827	2756	7.51	102.65	2.50	27.9	32.75
		17	2590	2385	7.83	164.17	4.00	26.1	33.70
		18	2354	2013	8.05	240.04	5.70	26.4	36.70
		19	2319	2051	7.94	192.93	4.59	26.5	36.60
		20	2357	2092	7.90	193.55	4.63	28.1	36.17
Agua	5.4	21	2444	2167	7.93	203.84	4.90	27.4	35.60
		22	2364	2128	7.87	176.51	4.27	28.0	35.10
		23	2314	2088	7.85	168.22	4.07	28.4	35.10
		24	2347	2063	7.95	206.13	4.98	28.2	35.10
		25	2363	2049	8.01	226.08	5.47	27.7	34.90
Mini	4.9	44	2443	2071	8.08	265.01	6.31	26.9	36.50
		45	2365	2113	7.90	184.16	4.37	26.6	36.90
		46	2356	2049	7.99	218.13	5.16	26.4	37.30

Source: PRODUCED BY THE AUTHOR, 2022

3.2.2 Foraminiferal analysis

The assemblages found at PM exhibit similar composition to previous studies conducted in nearby coastal settings (GISCHLER; MÖDER, 2009), Caribbean eastern islands (WILSON; WILSON, 2011), and the Gulf of Mexico (STEPHENSON; HALLOCK; KELMO, 2015; AMERGIAN *et al.*, 2022). A total of 8564 foraminifera from 141 species were identified, belonging to 4 orders, 37 families, and 73 genera (Appendix A). Agglutinated species contributed ~6.4% (9 species), porcelaneous 61% (86 species), and hyaline 32.6% (45 species) of the total species richness. The species *Ar. angulatus* (9.4%), followed by *Rotorbinella rosea* (9.3%), *Asterigerina carinata* (6.9%), and the *Rotorbis auberii* (4.7%) were the most important contributing taxa. Considering a 3% contribution cutoff, a total of 34 species were considered for the faunal analysis (Fig. 2).

Figure 2 – Electron micrographs of the species from Puerto Morelos reef lagoon springs considered for faunal analysis. Legend: ***1*** *Textularia agglutinans*, lateral view. **2** *Clavulina angularis*, lateral view. **3** *Valvulina oviedoiana*, lateral view. **4** *Spiroloculina corrugata*, lateral view. **5** *Agglutinella compressa*, lateral view. **6** *Schlumbergerina alveoliniformis*, lateral view. **7** *Lachlanella carinata*, lateral view. **8** *Quinqueloculina subpoeyana*, lateral view. **9** *Quinqueloculina tricarinata*, lateral view. **10a, 10c** *Quinqueloculina* conf. *Quinqueloculina distorqueata*, lateral views. **10b** *Quinqueloculina* conf. *Quinqueloculina distorqueata*, apertural view. **11** *Quinqueloculina bosciana*, lateral view. **12** *Quinqueloculina disparilis*, lateral view. **13** *Quinqueloculina* conf. Q. *berthelotiana*, lateral view. **14a,14c** *Quinqueloculina carinatastriata*, lateral views. **14b** *Quinqueloculina carinatastriata*, apertural view. **15a,15c** *Affinetrina quadrilateralis*, apertural views. **15b** *Affinetrina quadrilateralis*, apertural view. **16** *Miliolinella elongata*, lateral view. **17** *Pseudotriloculina linneiana*, lateral view. **18** *Articulina pacifica*, lateral view. **19** *Laevipeneroplis proteus*, lateral view. **20** *Peneroplis pertustus*, lateral view. **21** *Peneroplis planatus*, lateral view. **22** *Archaias angulatus*, lateral view. **23** *Cyclorbiculina compressa*, lateral view. **24** *Sorites marginalis*, lateral view. **25** *Rotorbis auberii*, spiral view. **26** *Rotorbinella rosea*, spiral view. **27** *Trochulina* sp, spiral view. **28** *Rosalina* cf. *floridana*, spiral view. **29** *Rosalina globularis*, spiral view. **30** *Cibicidoides* sp, spiral view. **31** *Planorbulina mediterranensis*, lateral view. **32** *Planogypsina acervalis*, lateral view. **33** *Amphistegina gibbosa*, lateral view. **34** *Asterigerina carinata*, lateral view. Scale bar represents 100 µm

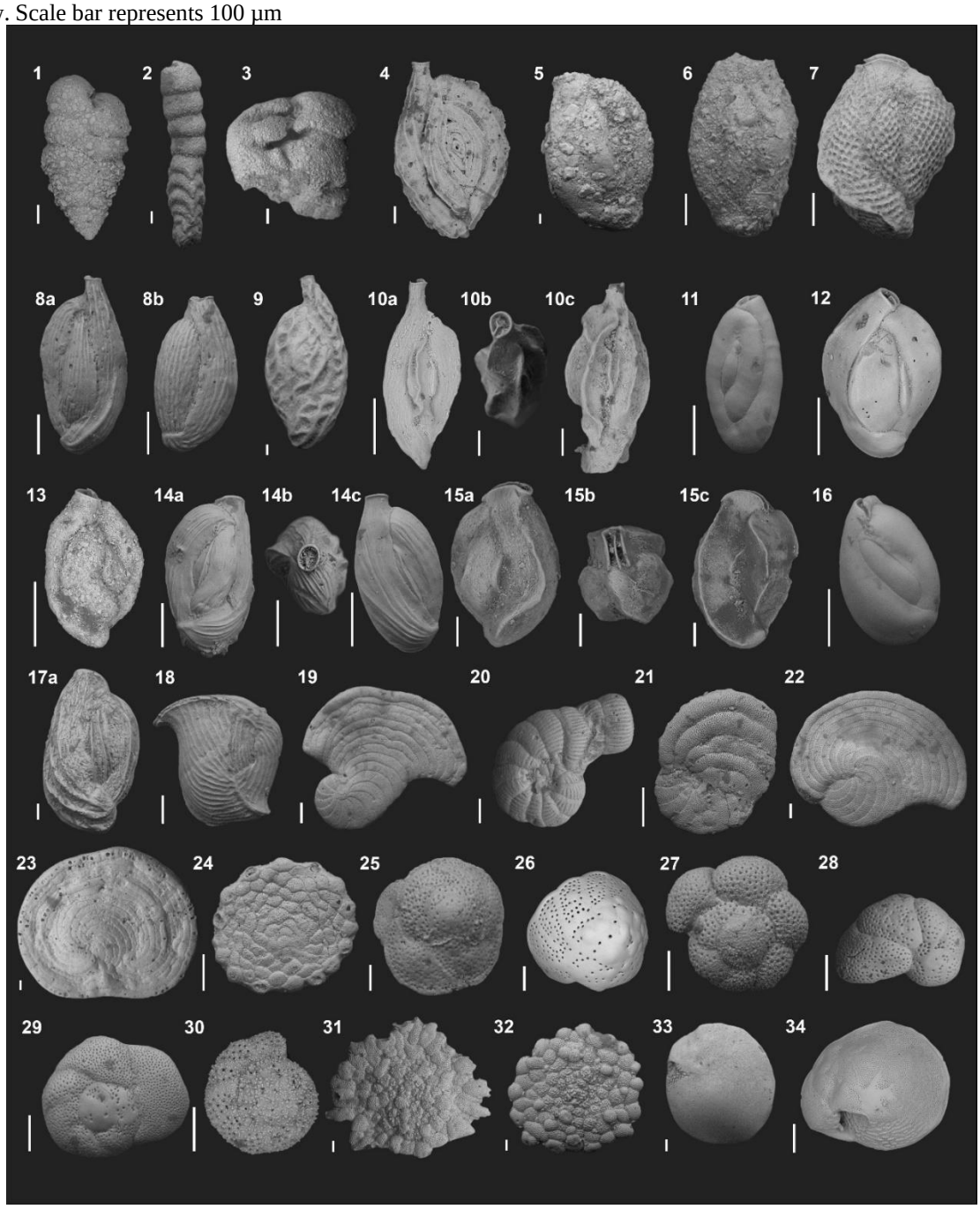

Source: PRODUCED BY THE AUTHOR, 2022

The relationship between water chemistry and species abundance can be visualized in the CCA diagram (Fig. 3), where a gradient of acidification stress is represented by Axis 1 (p-value = 0.001), which explains roughly 63% of the total variance. In CCA, the environmental variables are represented by vectors, and their length reflects the relative importance to species distribution. As observed in BIOENV and global BEST analysis, CCA also indicates that pH represents the most important variable to foraminifera distribution, while temperature the least. Species at the left side of Fig. 3 (e.g., *Quinqueloculina tricarinata*, *Ar. angulatus*, *Amphistegina gibbosa*, *Valvulina oviedoiana*, *Cyclorbiculina compressa*) increased towards low-pH, high C_T, and T_A values, presenting an increased abundance and lower sensitivity to OA. On contrary, sensitive species (e.g., *Thoculina* sp, *Sorites marginalis*, *Quinqueloculina subpoeyana*, *R. auberii*) are positioned at the right side of the plot (Fig. 3) close to high-pH, Ω Calcite and CO_3^{2-} values. The species *Rotorbinella rosea*, *Clavulina angularis*, *Quinqueloculina disparilis*, *Lachlanella carinata* and *Schlumbergerina alveoliniformis* present at the intermediated position in the graph decreased in abundance towards low-pH at a lower rate compared to the species on the right suggesting more tolerance. Axis 2 explained 19% of the total variance, however no significant correlation to species distribution was found (p-value = 0.1).

Figure 3 – Canonical correspondence analysis diagram of the foraminiferal species (>3%) in respect to water chemistry data (black). Legend: AQ = *A. quadrilateralis*, AC = *A. carinata*, AL = *A. gibbosa*, AA = *Ar. angulatus*, AP = *A. pacifica*, AC = *A. compressa*, CI = *Cibicidoides* sp, CA = *C. angularis*, CC = *C. compressa*, LC = *L. carinata*, LP = *L. proteus*, ME = *M. elongata*, PPE = *P. pertustus*, PP = *P. planatus*, PA = *P. acervalis*, PM = *P. mediterranensis*, PL = *P. linneiana*, QBO = *Q. bosciana*, QC = *Q. carinatastriata*, QB = *Q. berthelotiana*, *QD* = *Q. distorqueata*, QDI = *Q. disparilis*, QS = *Q. subpoeyana*, QT = *Q. tricarinata*, RF = *R. floridana*, RG = *R. globularis*, RR = *R. rosea*, RA = *R. auberii*, AS = *S. alveoliniformis* , SM = *S.marginalis*, SC = *S. corrugata*, TA = *T. agglutinans*, TRO = *Trochulina* sp,VO = *V. oviedoiana*, Calcite = Ω Calcite, CO3 = CO_3^{2-a}, Te = temperature

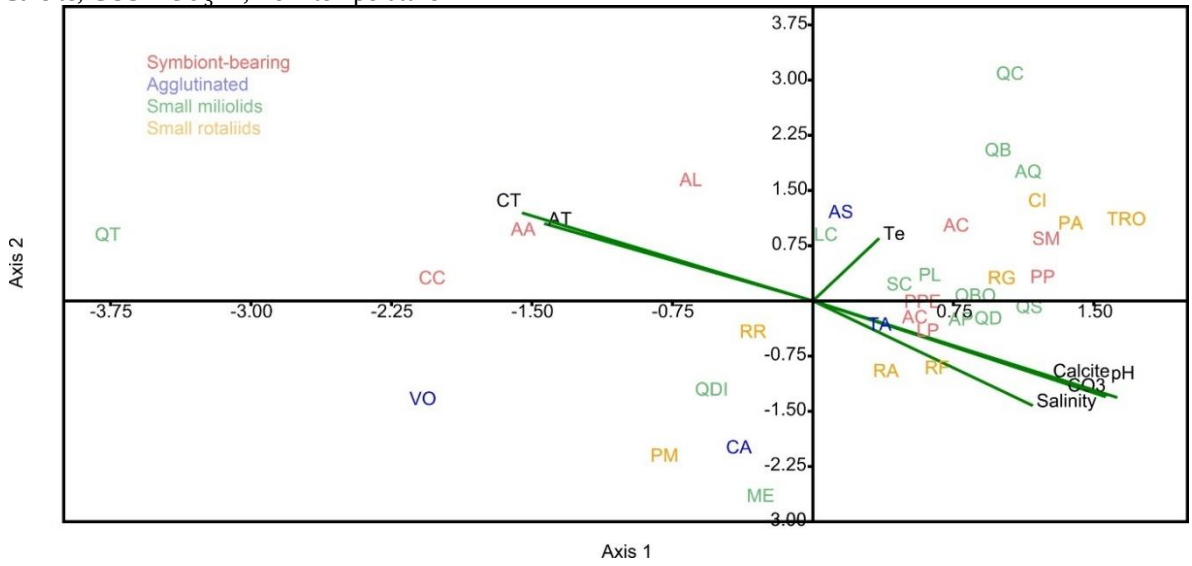

The distribution of functional groups against changing pH is represented in Fig. 4. The symbiont-bearing taxa (Fig. 4A, R^2 = 0.54, p-value = 0.00) presented lower sensitivity to OA conditions, increasing in relative abundance towards low-pH. The smaller miliolids (Fig. 5C, R^2 = 0.42, p-value = 0.00), opportunistic (Fig. 4D, R^2 = 0.28, p-value = 0.00), and smaller rotaliid taxa (Fig. 4A, R^2 = 0.36, p-value = 0.00) decreased in relative abundance towards low-pH conditions, presenting higher sensitivity. Kruskal-Wallis analysis reveal that the observed variation was statistically significant for most taxonomic metrics: Symbiont-bearing (chi-squared = 13, df = 3, p-value = 0.00), smaller miliolids (chi-squared = 12, df = 3, p-value = 0.00), opportunistic (chi-squared = 16, df = 3, p-value = 0.00), and smaller rotaliid (chi-squared = 9, df = 3, p-value = 0.00) and H (chi-squared = 19, df = 3, p-value = 0.00). Specifically, post hoc Dunn test revels that the significant changes occurred mainly between present day (~ 8.1 pH units) and extremely low-pH conditions (≤ 7.6 pH units) representing conditions beyond those predicted by the end of 21st century: Symbiont-bearing (z = −2.38, p-value = 0.01), smaller miliolids (z = 2.7, p-value = 0.00), and opportunistic (z= 2.4, p-value = 0.01). For smaller rotaliid taxa the significance was observed between low-intermediate acidification scenarios (~7.9 pH units), at which the group presented a higher contribution, and extremely low-pH conditions (≤ 7.6 pH units) where a strong decrease was observed with the other metrics (z = 1.7, p-value = 0.00). No significance was observed for agglutinated foraminifera (chi-squared = 2, df = 3, p-value = 0.5), which also did not present significant correlation with changing pH (Fig. 4E, R^2 = 0.11, p-value = 0.1). Raw data of functional and test type group are presented in Appendix B.

Figure 4 – Variation of functional groups against changing pH. The black line represents the second-order polynomial model fits along with the R^2 value and the blue line represents the raw values obtained from in situ assemblages. Dashed lines demark predicted pH values at the end of this century following the Coupled Model Intercomparison Project Phase Six (CMIP6) predictions for Shared Socioeconomic Pathways (SSP1-2.6: 8.01 pH units; SSP2-4.5: 7.91 pH units; SSP3-7.0: 7.82 pH units, and SSP4: 7.73 pH units)

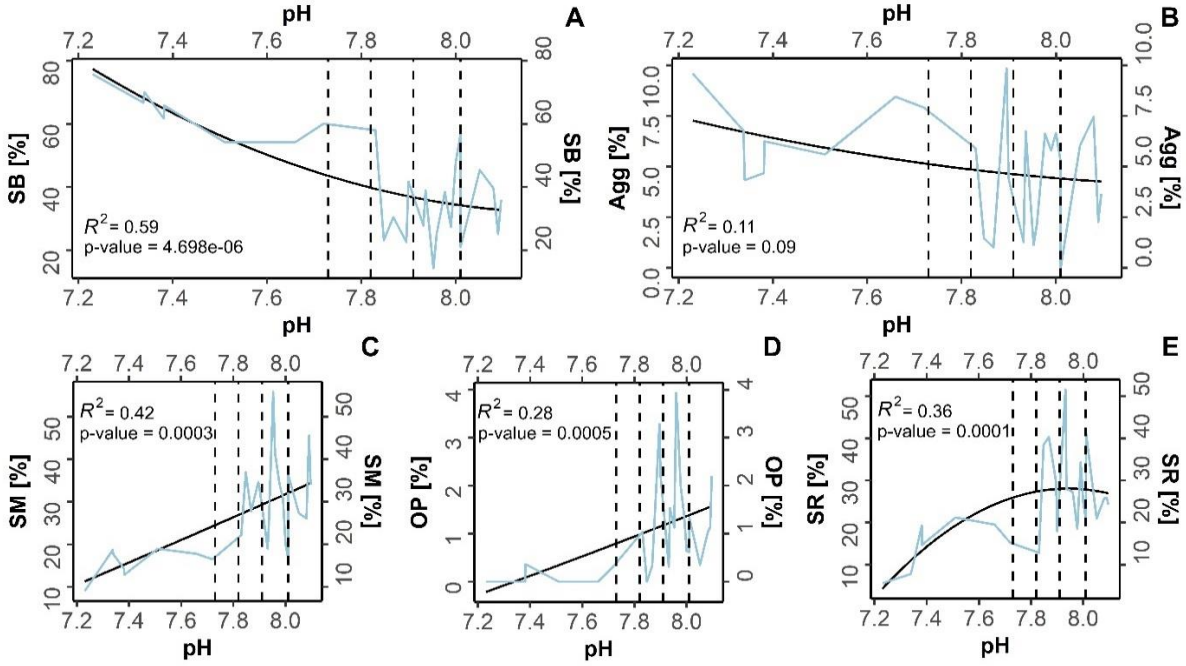

Source: PRODUCED BY THE AUTHOR, 2022.

All taxonomic metrics presented a gradual decrease towards low-pH waters. On average, H′ ranged from 3.9 to 1.6 (Fig. 5A, R^2 = 0.72, p-value = 4.8^{-08}); S from 71 to 11 (Fig. 5B, R^2 = 0.67, p-value = 3.3^{-07}); J' from 0.9 to 0.6 (Fig. 5C, R^2 = 0.64, p-value = 9.5^{-07}), and foraminifera density from 2167 to 36 ind./ml (Fig. 5D, R^2 = 0.22, p-value = 0.02). Kruskal-Wallis analysis revealed that the observed variation was statistically significant for all taxonomic metrics: N (chi-squared = 14.5, df = 3, p-value = 0.00), S (chi-squared = 20, df = 3, p-value = 0.00), J' (chi-squared = 15, df = 3, p-value = 0.00) and H (chi-squared = 19, df = 3, p-value = 0.00). However as observed for functional and test type groups, the post hoc Dunn test revealed that significant changes occurred mainly between present day and extremely low-pH conditions: N (z = 2.2, p-value = 0.02), S (z = 3.4, p-value = 0.00), J (z = 3.1, p-value = 0.00), and H (z= 3.4, p-value = 0.00). No significant difference was observed for low-intermediate acidification scenarios (SSP1-2.6 and SSP2-4.5), and only S differed significantly between present day and high acidification scenarios (Fig. 5B, SSP3-7.0 and SSP5-8.5, z = 2.1, p-value = 0.03).

Figure 5 – Relationships between pH and (A) Shannon-Weiner Diversity Index, (B) foraminiferal density, (C) Pielou's evenness, and (D) species richness. The black lines represent second-order polynomial model fits, and grey areas mark 95% confidence intervals. Dashed lines demark predicted pH values at the end of this century following the Coupled Model Intercomparison Project Phase Six (CMIP6) predictions for Shared Socioeconomic Pathways (SSP1-2.6: 8.01 pH units; SSP2-4.5: 7.91 pH units; SSP3-7.0: 7.82 pH units, and SSP4: 7.73 pH units)

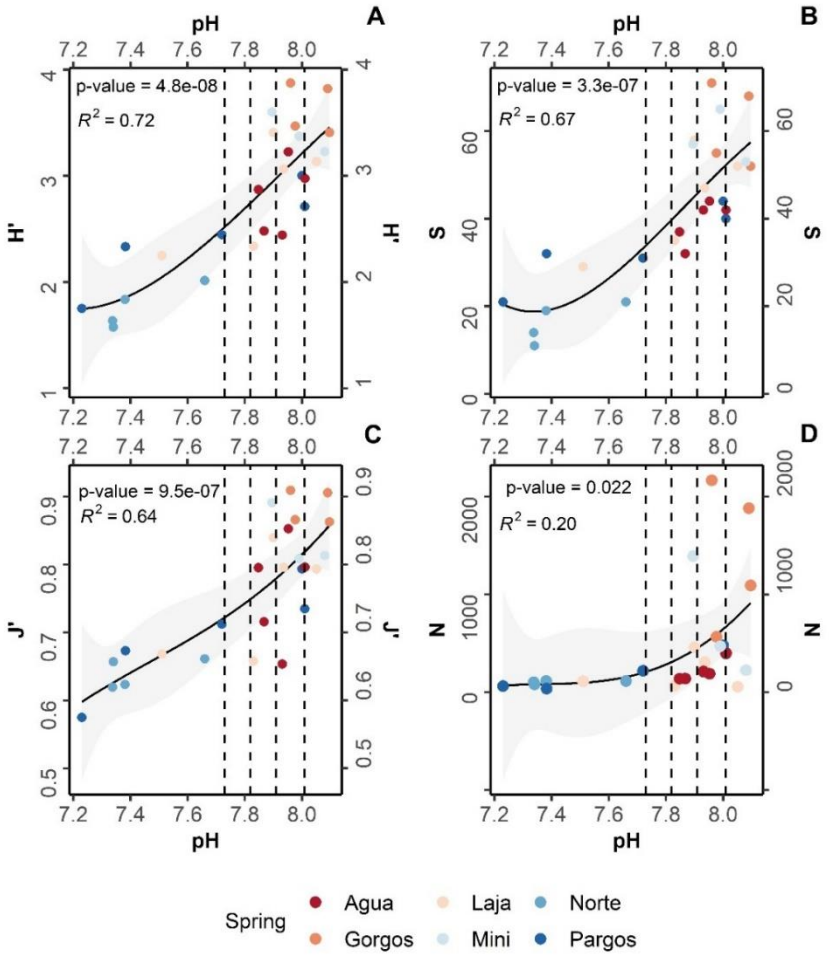

Source: PRODUCED BY THE AUTHOR, 2022

The hierarchical clustering based on foraminifera abundances revealed 7 assemblages, which corresponded well to functional and test-type group distributions (Fig. 4), changes in carbonate water chemistry (Table 1) and taxonomic metrics (Fig. 5). A good representation of assemblage groups' structure is present in nMDS plot (Fig. 6, 2D Stress: 0.06). Assemblages "f" and "e" consisted of samples retrieved at the higher pH conditions (8.1–7.9 pH units). Assemblages "g" and "d' comprised samples retrieved at intermediate pH conditions (8.08–7.72 and 8–7.85, respectively). Assemblage "c" and assemblages "b" and "a" samples retrieved at extremely low-pH conditions of 8–7.51 and 7.66–7.23, respectively. The reduction of diversity, richness, and evenness along with decreasing pH can be observed from the left to the right part of the diagram (Fig. 6). An increase in symbiont-bearing and decrease in other groups also occurs towards the right part of the plot. SIMPER analysis reveals that the species *Ar. angulatus*, whose relative contribution increased towards low-pH

conditions, was the major contributor to the forming groups, except assemblages “e” and “f” that were dominated by sensitive species that did not occur at low-pH (e.g., *Throculina* sp, *Sorites marginalis*, *Quinqueloculina subpoeyana*, *R. auberii*). All species that are predominantly responsible for each group are listed in Appendix C.

In comparison to future projections, the highest dissimilarity (> 80%) was observed between assemblages living close to present-day conditions (assemblage “e”) and at the center of discharge, representing conditions beyond those projected for the end of the 21st century (assemblages “a” and “b”). Moderate similarity (47%) was still observed for samples living at present-day (8.1 pH units), low-intermediate acidification (~ 7.9 pH units, SSP1-2.6 and SSP2-4.5), and high acidification scenarios (7.8-7.7 pH units, SSP3-7.0 and SSP5-8.5).

Figure 6 Non-metric multidimensional scaling (nMDS) ordination plot of 26 sampling stations of benthic foraminifera from Puerto Morelos

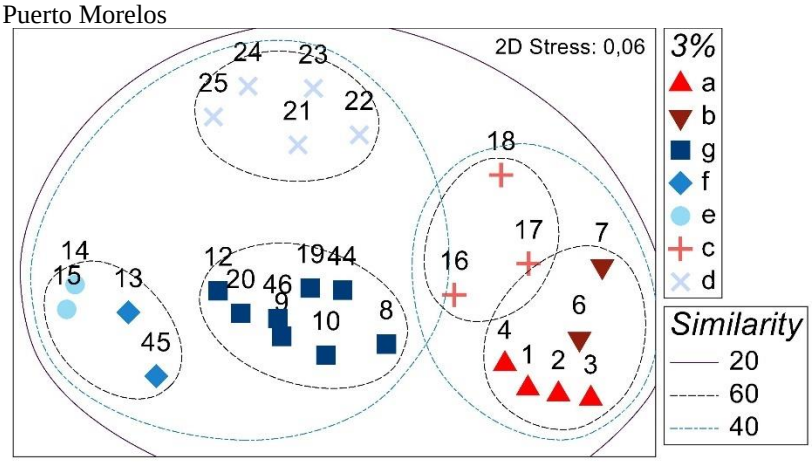

Source: PRODUCED BY THE AUTHOR, 2022.

Considering the consistency in the data analyses, we observed that under the most conservative projections (SSP1-2.6; SSP2-4.5) foraminiferal assemblages did not display considerable changes in taxonomic metrics, presenting a moderate similarity (~50%) to assemblages living at present-day conditions. For projections SSP3-7.0 and SSP5-8.5, moderate similarity was also observed, but the analyzed assemblages presented a significant decrease in richness S, indicating that foraminifera communities are likely to be affected under high acidification scenarios. To a species level, the symbiont-bearing taxa presented relatively higher resistance when compared to other functional groups, while agglutinated foraminifera were not measurably influenced by changes in pH.

3.2.1 Taphonomical and assemblage test-size analysis

High-pH stations (~8.1 pH units) at PM are relatively pristine, however, this gradually changes as the effects of exudated waters increase. Linear correlations (Fig. 7B) show that dissolution (R^2 = 0.55, p-value = 0.00), and to a lesser extent, breakage (R^2 = 0.30, p-value = 0.00), increased with reducing pH until 7.8 units, where high levels of taphonomical alteration stated to occur. In respect to species distribution, the regression analysis shows a high correlation between the occurrence of some species and changing pH. Specifically, *Ar. angulatus* was responsible for 73% of the dissolution observed in the samples (R^2 = 0.73, p-value = 0.00).

Along the gradient of changing carbonate chemistry, a significant change in foraminiferal assemblage test size was observed (Kruskal-Wallis, chi-squared = 16, df = 3, p-value = 0.00). A gradual decrease in the abundance of tests with smaller surface area and a relative increase of larger tests is observed towards low-pH sites (Fig. 7, R^2 = 0.73, p-value = 0.00). The post hoc Dunn's test reveals that only the differences between present-day and extremely low-pH conditions, which are beyond the predicted to the end of the 21st century were significant (z = −2.7, p-value = 0.00). Specifically, average test size in the assemblage more than tripled when compared to present-day conditions (from 0.33 ± 0.2 to 0.87 ± 0.14 mm^2). This abrupt change can be visualized in Fig. 6A, likely responding to changes in faunal composition rather than interspecific changes in species size. As observed in taphonomical analysis, linear correlation with respect to dominant taxa coverage (i.e., the species *Ar. angulatus*) shows a high and significant correlation of this species to changes in average assemblage test size (Fig. 7C, R^2 = 0.89, p-value = 0.00). Raw data of assemblage average test size, and diverse analysis are available in Appendix D.

Figure 7 – The (A) density plot of assemblage test size, (B) variation of dissolution and breakage against changing pH, and (C) variation of dissolution and average assemblage test size against *Archaias angulatus* relative contribution. The black lines represent second-order polynomial model fits along with the R^2 value and p-value (B; C). Dashed lines demark stations under high taphonomical alteration

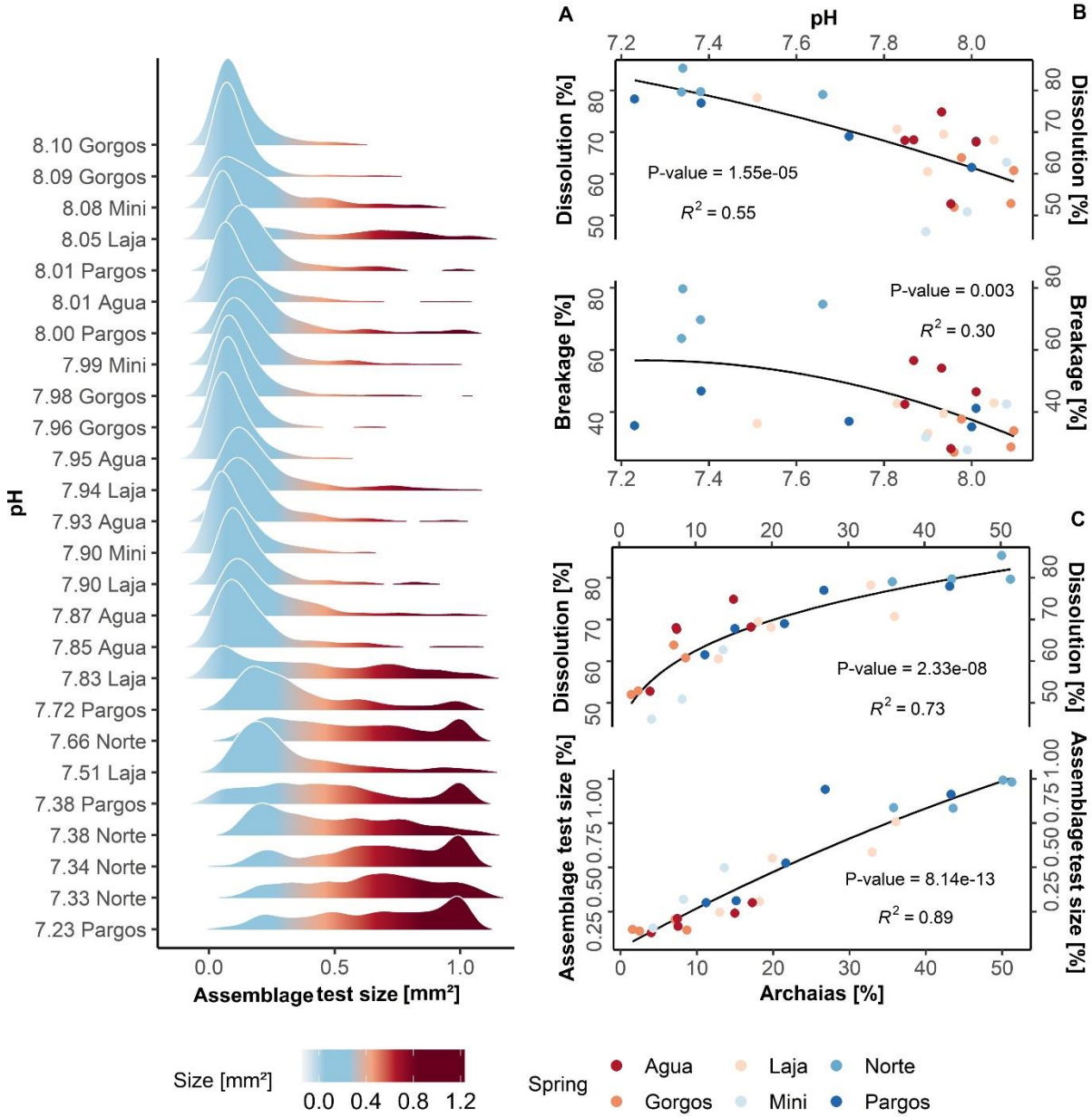

Source: PRODUCED BY THE AUTHOR, 2022.

3.2.4 X-ray MicroCT

The X-ray MicroCT (Fig.8A−D) analysis revealed that despite having a similar size (0.80 ± 0.05 mm^3) and volume (0.06 ± 0.02 mm^3), the specimens present at low-pH conditions (7.11 pH units) were on average 46% less dense (2.40 ± 0.2 to 1.30 ± 0.03 g/cm^3) than the specimens present at high-pH conditions (Welch Two Sample t-test, t = 8.1204, df = 3.0808, p-value = 0.0035). Yet, no significant (Two Sample t-test, t = −1.4378, df = 6, p-value

= 0.2) difference in chamber wall thickness was observed (0.050 ± 0.006 mm^3). The differences in internal density can be seen in fig. 8A and 8B representing 2 specimens living in high and low-pH conditions, respectively. The external differences of these same individuals are represented in the 3D volume rendering at Fig. 8C and 8DRaw data of test density, chamber wall thickness, test volume, and test diameter measured in *Ar. angulatus* individuals are listed in Appendix E.

Figure 8 – Comparison between X-ray microCT images with color code as a function of calcite density. The specimen living at ~ 7.96 pH units (A) presents a higher calcite density when compared with low ~ pH 7.11 individual (B). The 3D Volume rendering in function of calcite density for the same individuals living at the high (C) and low-pH conditions (D). Note that individual at D the individual living under low-pH presents a test with incomplete parts and blurred edges, demonstrating lower density

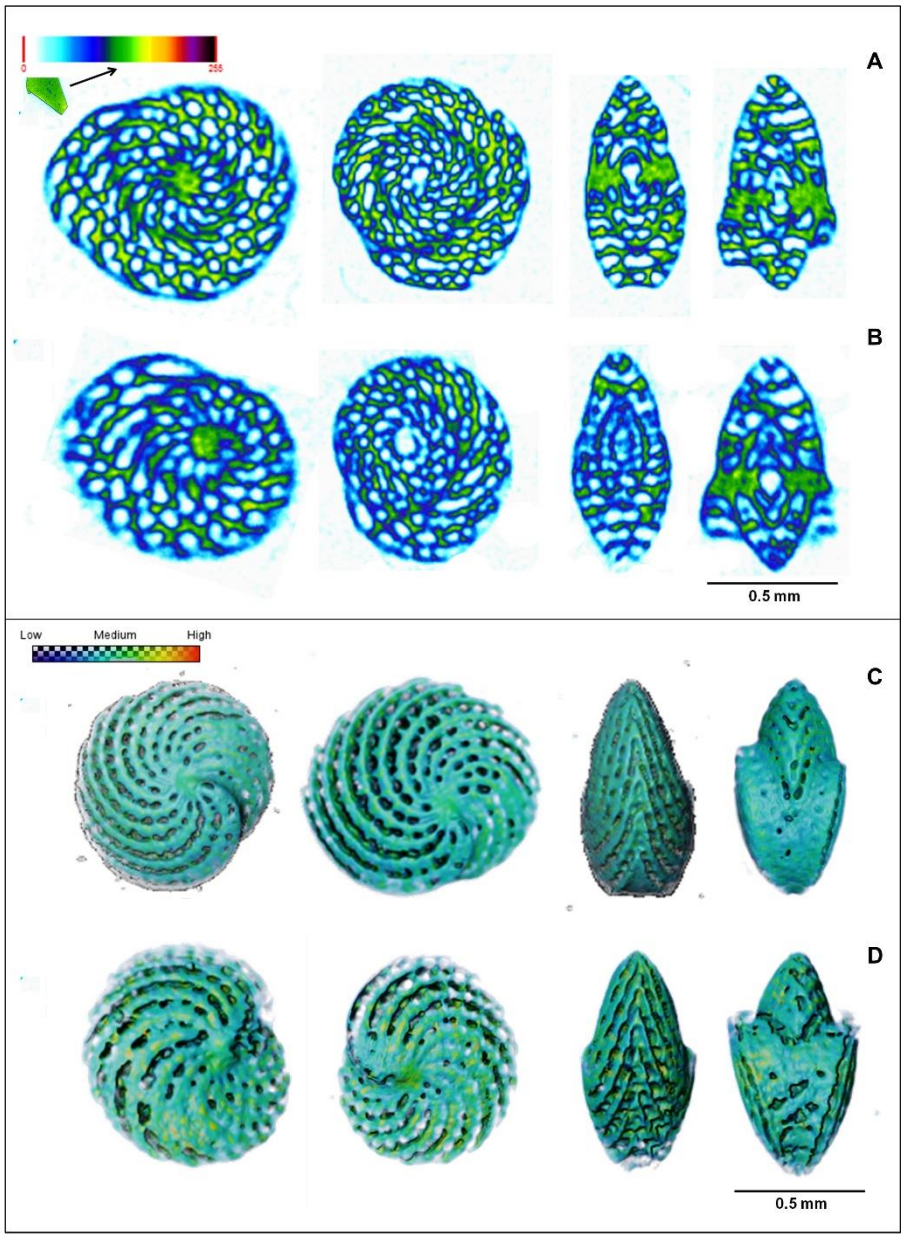

Source: PRODUCED BY THE AUTHOR, 2022.

3.3 Discussion

Under the two most conservative acidification projections (Fig. 5A–D) foraminiferal assemblages in PM did not display considerable changes, while at high acidification scenarios a significant decrease in species richness was observed. These results indicate that benthic foraminifera are unlikely be affected by pH decreases of ~0.2, but certainly respond adversely to higher acidification levels (~0.4 pH units). These findings are consistent with previous observations from other naturally high pCO_2 sites in which taxonomic metrics decreased significantly with declining pH (BERNHARD *et al.* 2009; DIAS *et al*. 2010; PETTIT *et al.*, 2015; DONG *et al*., 2019, 2020). It is noteworthy, however, that changes in assemblage composition did not follow the same pattern observed in these previous studies. Whereas the proportion of calcareous species usually decline with decreasing pH, they remained dominant (~90%) under all projections in PM, suggesting a relatively higher resistance for these shallow-reef benthic communities.

The in-situ occurrence of calcifying foraminifera at high acidification scenarios (SSP3-7.0 and SSP5-8.5) have only been reported in the deep-sea near extensive CO_2 vents in the Wagner Basin (PETTIT *et al.*, 2013). At this site, a rich food supply and stable temperatures were considered to offset the effects of OA and a shift towards opportunistic communities was reported. The springs from PM also have high nutrient concentrations compared to the open waters in the region (NULL *et al.*, 2014; CROOK *et al.*, 2016), however, near spring assemblages did not change towards opportunistic dominated assemblages, suggesting that the nutrient availability does not exert a major control at this site. Rather, the high-pH assemblages heavily dominated by small calcareous forms were replaced by larger symbiont-bearing species near the springs (Fig. 4A-E). Symbiont-bearing species are known to be sensitive to high nutrient loading, likely because of changes in turbidity/light regimes because of their dependence on algal symbionts to enhance growth and calcification (HALLOCK *et al.*, 2003). At PM despite higher nutrient levels the waters at the springs are clear and light regimes are not reduced.

The chemical conditions at PM, along with the physiology of calcification in foraminifera, may also explain the lack of sensitivity to the mid-range pH conditions. Recent calcification models demonstrate that foraminifera are able to manipulate pH to control the speciation of inorganic carbon parameters during calcification (DE NOOIJER *et al.*, 2009; TOYOFUKU *et al.*, 2017; DE GOYESE *et al.*, 2021; GEERKEN *et al.*, 2022). Specifically, the proton-pumping based model (TOYOFUKU *et al.*, 2017) shows that at the external environment, a decrease in pH (~6.9 pH units) induces the transformation of CO_3^{2-} and

bicarbonate (HCO^{3-}) into CO_2, whereas at the site of calcification the elevated pH (~9 pH units) results in the opposite shift into CO_3^{2-}. As foraminifera induce pH changes exceeding the predicted to SSP1-2.6 and SSP2-4.5, low-intermediate acidification scenarios are in fact unlikely to impair foraminiferal calcification. As such, these models also suggest that increased CO_2 might favor foraminifera by increasing C_T, which is notably higher towards the springs in PM (Table 1).

It is also suggested that higher C_T might favor symbiont-bearing foraminifera at low-pH (~ 7.8) by inducing CO_2 fertilization effects and increased activity of symbionts (FUJITA *et al.*, 2011), which is in agreement with our results. For example, from assemblage e and f (~ 8.1 pH units) to g and d (~7.7 pH, SIMPER analysis) symbiont-bearing species including (1) *Ar. angulatus* (chlorophyte-bearing), increased in abundance from 4–7% to 10–13%, (B) *Amphistegina lessonii* (diatom-bearing), increased in some stations from 4% to 7%, and (C) *Cyclorbiculina compressa* (chlorophyte-bearing) that presented low contribution < 3% at high-pH stations also increased in relative contribution to 4% at intermediated pH. Additionally, the high C_T and T_A might also raise local pH and carbonate saturation during photosynthesis, even if only on the scale of an individual organism at the foraminiferal shell surface, which could also increase the symbiont-bearing resistance. Under ambient conditions, Köhler-Rink and Kühl (2000) observed that photosynthesis increased the pH up to 8.6. These species were also placed close to the C_T vector at the CCA diagram, which highlights their association to higher dissolved carbon content (Fig. 3). In accord, laboratory-controlled experiments have also shown that the symbiont-bearing *Ar. angulatus* (STUHR *et al.*, 2021) and *Amphistegina* sp. (PRAZERES *et al.*, 2015) can calcify and live under relatively low-pH conditions (~ 7.6 pH units).

The ability of foraminifera to function and calcify near the springs may also be related to the site-specific natural pH variability to which the community is exposed. For example for many coastal/transitional areas characterized by high pCO_2 variability foraminifera seem to be more resilient and acclimated to changing conditions including low-pH (HAYNERT *et al.*, 2012; CHARRIEAU *et al.*, 2018). By discharging low-pH waters for millennia (BACK *et al.*, 1979) the foraminifera living near the spring have experienced a pH variability over a much longer timespan than the life span of individual organisms (MARTINEZ *et al.*, 2018). Specifically, as reef-dwelling organisms, the foraminifera in PM experience a wide range of pH on daily and seasonal scales which might, at least to a certain extent, physiologically increase the species resilience to low-pH waters (PRICE *et al.*, 2012). Moreover, in-situ recruitment and succession experiments in PM showed that foraminifera

were able to calcify and increased in density over the investigated period (14 months) (data from Laja and Gorgos springs , CROOK *et al.,* 2016). As observed by Martinez *et al.* (2018) calcareous species at PM persist even at extreme acidification levels (~ 7.1 pH units).

In our work we observed that *A.angulatus* doubled its relative contribution at low-pH (~8–7.8) (e.g., 13% in assemblage "g", Appendix C) and almost tripled at extremely low-pH (>7.7) (e.g., 30% in assemblage 'a", Appendix C) compared to assemblages living at 8.1 pH units (e.g., 4% in assemblage "e", Appendix C). Due to its strong increase towards the springs, we employed an X-ray microCT analysis (Fig. 8A-D) to investigate possible acclimation patterns that could explain the observation.

The analysis revealed that despite having similar size (0.80 ± 0.05 mm^3), volume (0.06 ± 0.02 mm^3), and chamber wall thickness(0.050 ± 0.006 mm^3), the specimens found at low-pH conditions (7.11 pH units) were on average 46% less dense (2.40 ± 0.2 to 1.30 ± 0.03 g/cm^3) than the specimens present at high-pH conditions (7.96 pH units). This demonstrates that the species is able to calcify in low-pH conditions beyond the predicted for the late 21st century albite at lower density. The lower density however indicates that *Archaias* individuals were not capable to acclimate sufficiently to maintain ambient present day calcification efficiency. These results are in agreement with Knorr *et al.* (2015) that observed a 50% decrease in *Ar. angulatus* size at 7.6 pH units, and a consequent decrease of 85% in the production of high-Mg calcite by this species. Further analyses are needed for a better understanding of *Archaias* biological thresholds, but this ability to calcify at even 7.11 pH units certainly provides a competitive advantage over other species that are less robust calcifiers.

Considering that foraminifera are a crucial component of reef sediment production (LANGER *et al.,* 1997; LANGER, 2008), including *Ar. angulatus* in the Caribbean region, our results support previous findings that reef-building carbonate production and accumulation are likely to decrease under future scenarios, even in the tropics (EYRE *et al.,* 2018; KUROYANAGI *et al.,* 2021, AMERGIAN *et al.,* 2022). Specifically, we also observed a decrease in foraminifera density (Fig. 5D) and therefore in carbonate accumulation as foraminiferal tests in the sediments. As OA intensifies, symbiont-bearing taxa, which demonstrated higher resistance to low-pH, will likely still represent major contributors in the Caribbean and Gulf of Mexico sediments where species like *Ar. angulatus* dominate (CULVER; BUZAS, 1982). In contrary, the high sensitivity of *Rosalina* spp., *Quinqueloculina* spp., *Triloculina* spp., *Articulina* spp., and *Miliolinella* spp. to low-pH

highlighted their lower fitness in response to OA, demonstrating that changes in abundance of small taxa can be used as bioindicators to monitor the effects of OA.

Since *Ar. angulatus* showed lower density close to the low-pH springs and hence is negatively impacted by the low-pH, the species relative increase in contribution towards the springs is probably associated with the high preservation potential of its tests. Their tests are larger, thicker, and reinforced by internal partitions (pillars), therefore more likely to be preserved in the sediment (MARTIN, 1986; COTTEY; HALLOCK, 1988). This is confirmed by the performed regression analysis as the species relative contribution explains 88% of assemblage test size and 73% of dissolution occurrence in the samples (Fig. 7C). In fact, changes were so abrupt that shifts in the assemblages' test size and functional groups were clearly observed at ≤ 7.83 pH units (Fig. 7A), when the symbiont-bearing taxa contribution also started to increase (Fig. 4A). At this point biological thresholds of smaller taxa seemed to be crossed, and their relative decrease near the springs is likely related to their low density and hence higher rates of breakage and dissolution (Present study, MARTINEZ *et al.*, 2018).

The relative contribution of agglutinated foraminifera slightly increased towards low-pH (Fig. 4B), but they did not compensate for the decline in calcareous species (Fig. 4A–E). Since the particles available for the agglutinated tests are made of carbonate and, under low-Ω waters are also prone to dissolve, that may affect the agglutinated species. Interestingly, agglutinated foraminifera also presented species-specific responses to acidification similar to the calcareous foraminifera. For example, *Valvulina oviedoiana* increased towards low-pH while *Textularia agglutinans* presented a strong decrease. Since acidification is expected to have little direct effect on agglutinated foraminifera the observed interspecific behavior is also probably associated with preservation potential. The variation of agglutinating material (e.g., mucopolysaccharide), structure (e.g., fibrous, strands, foam-like masses), and size of granular particles (e.g., fine, and coarser) are essential to determine the preservation and accumulation of agglutinated tests (BENDER; HEMLEBEN, 1988). The most important agglutinated species, in our study e.g., *T. agglutinans*, *C. angulata*, and *V. oviedoiana* use calcitic cement as the agglutinating material of particles, which probably assigns a higher resistance to dissolution (BENDER, 1995). Among these, *T. agglutinans* lower resistance likely responds to its smaller size and higher internal pore diameter, which implies higher dissolution (BENDER, 1995). Altogether, we observe that until ~ 7.8 pH units foraminifera physiology was a main driver of foraminifera distribution, whereas at ≤ 7.7 pH units (Fig. 7B) the preservation potential became an important factor affecting the distribution of both calcareous and agglutinated tests.

Although *postmortem* degradation likely occurs at higher rates near the springs, the distribution of species still provide a good representation of the fauna over a short ecological time. That is also the case for most symbiont-bearing taxa, as the relative contribution of individual species discussed above increase towards low-pH. However, we cannot exclude the possibility that a higher accumulation of *Ar. angulatus* test could be responsible for an overestimation in symbiont-bearing taxa density. In this case, species richness would be more reliable to the interpretation of the community responses, which was the only parameter to decrease significantly at < 7.7 pH units (Fig. 5B), validating that, in general foraminifera, are less likely to acclimate under high acidification scenarios. These results bring serious implications as SSP3-7.0 and SSP5-8.5 scenarios also predict substantial increases of sea surface temperature (KWIATKOWSKI *et al.*, 2020), which combined to surface OA might critically decrease the tolerance of foraminifera species (reviewed in KAWAHATA *et al.*, 2019). Recently, Bernhard *et al.* (2021) observed that foraminiferal assemblages presented the lowest number of species and abundances under a triple-stressed (low-pH/O_2 and high temperature) treatment, demonstrating the synergetic effects of these variables. As observed in PM, agglutinated foraminifera were relatively more resistant than calcareous taxa.

For emissions beyond the predicted to the end of 21st century, all taxonomic metrics decreased significantly, and calcareous species with higher preservation potential like *C. compressa* and *Ar. angulatus* comprised up 50–60 % of assemblage composition. These calcareous taxa were still found probably due to high TA levels, which was also considered to likely limit the dissolution rates of Ar. angulatus and other porcelaneous tests in the springs coast of Florida, where numerous spring-fed rivers emerge from Eocene and Oligocene limestone and dolostone substrata (AMERGIAN *et al.*, 2022). If we restricted the analysis to only pristine, well-preserved tests, the taxonomic metrics at 7.6–7.2 (Fig. 6) would be much lower than H' ~ 2 and more similar to those presented by Uthicke, Momigliano and Fabricius (2013), in which foraminifera were almost absent at sites with ≤ 7.9 pH units.

4 CONCLUSION

This work shows that despite their life-long exposure to low-pH conditions, tropical foraminifera species will be negatively affected under the high acidification scenarios (SSP3-7.0 and SSP5-8.5) for the end of the 21st century. Species-specific responses in foraminiferal assemblages were observed and as the oceans become more acidic, reef foraminiferal communities might gradually shift towards larger, symbiont-bearing species and agglutinating foraminifera. The species *Ar. angulatus*, which is known to be dominant in warm, oligotrophic areas of the Caribbean and Gulf of Mexico, are able to calcify at pH conditions lower than those projected by SSP5-8.5, however, the observed lower density of the pristine tests suggests that reef carbonate budget might decrease as this species represent a major carbonate producer at these areas. Considering the observed trends of increasing average assemblage test size and the results of multivariate faunal analysis (SIMPER, CCA), our results demonstrate the key role smaller foraminifera have as bioindicators to monitor the effects of OA, as their high sensitivity to dissolution makes them first responders to ongoing OA.

REFERENCES

ABU-ZIED, R. H.; AL-DUBAI, T. A.; BANTAN, R. A. Environmental conditions of shallow waters alongside the southern Corniche of Jeddah based on benthic foraminifera, physico-chemical parameters and heavy metals. **Journal of Foraminiferal Research**, v. 46, n. 2, p. 149–170, 2016. Available in: https://doi.org/10.2113/gsjfr.46.2.149. Access in: 20/jan. 2022.

AMERGIAN, K. E.; BECKWITH, S.; GFATTER, C.; SELDEN, C.; HALLOCK, P. Can areas of high alkalinity freshwater discharge provide potential refugia for marine calcifying organisms?. **Journal of Foraminiferal Research**, v. 52, n.1, p. 63–76, 2022. Available in: https://doi.org/10.2113/gsjfr.52.1.60. Access in: Access in: 25 jan. 2022.

ANDERSSON, A. J.; KLINE, D. I.; EDMUNDS, P. J.; ARCHER, S. D.; BEDNARSEK, N.; CARPENTER, R. C.; CHADSEYM M.; GOLDSTEIN, P.; GROTTOLI, A. G.; HURST, T. P.; KING, A. L.; KUBLER, J. E.; KUFFNER, I. B.; MACKEY, K. R. M.; MENGE, B. A.; PAYTAN, A.; RIEBESELL, U.; ZIMMERMAN, A. S. R. Understanding ocean acidification impacts on organismal to ecological scales. **Oceanography**, v. 28, n. 2, p. 16–27, 2015. Available in: https://doi.org/10.5670/oceanog.2015.27. Access in: 15 dec. 2022.

BACK, W.; HANSHAW, B. B. Comparison of chemical hydrogeology of the carbonate peninsulas of Florida and Yucatan. **Journal of Hydrology**, v. 10, p. 330–368, 1970. Available in: https:// doi.org/10.1016/0022-1694(70)90222-2. Access in: 10 dec. 2021.

BACK, W.; HANSHAW, B. B.; PYLE, T. E.; PLUMMER, L. N.; WEIDIE, A. E. Geochemical significance of groundwater discharge and carbonate solution to the formation of Caleta Xel Ha, Quintana Roo, Mexico. **Water Resources Research**, v. 19, n. 6, p. 1521–1535, 1979. Available in: https://doi.org/10.1029/WR015I006P01521. Access in: 12 dec. 2021.

BARBOSA, C. F.; FERREIRA, B. P.; SEOANE, J. C. S.; OLIVEIRA-SILVA, P.; GASPAR, A. L. B.; CORDEIRO, R. C.; SOARES-GOMES, A. Foraminifer-based coral reef health assessment for southwestern Atlantic offshore archipelagos, Brazil. **Journal of Foraminiferal Research**, v. 42, n.2, p. 169–183, 2012. Available in: https://doi.org/10.2113/gsjfr.42.2.169. Access in: 10 nov. 2021.

BARBOSA, C. F.; PRAZERES, M.; PADOVANI, B.; SEOANE, J. C. S. Foraminiferal assemblage and reef check census in coral reef health monitoring of East Brazilian margin. **Marine Micropaleontology**, v. 73, p. 62–69, 2009. Available in: https://doi.org/10.1016/j.marmicro.2009.07.002. Access in: 10 nov. 2021.

BEDDOWS, P. A.; SMART, P. L.; WHITAKER, F. F.; SMITH, S. L. Decoupled fresh – saline groundwater circulation of a coastal carbonate aquifer: Spatial patterns of temperature and specific electrical conductivity. **Journal of Hydrology**, v. 346, p. 18–32, 2007. Available in: https://doi.org/10.1016/j.jhydrol.2007.08.013. Access in: 7 dec. 2021.

BENDER, H. Test structure and classification in agglutinated Foraminifera. *In*: KAMINSKI, M. A.; GEROCH, S.; GASIÑSKI, M. A. (ed.). INTERNATIONAL WORKSHOP ON AGGLUTINATED FORAMINIFERA, 4., 1993, Kraków Poland. **Proceedings**… Kraków Poland, September 12-19, 1995. p. 27–70. (Grzybowski Foundation Special Publication, 3).

BENDER, H.; HEMLEBEN, C. Constructional aspects in test formation of some agglutinated foraminifera. **Abh. Geol. B.-A**., p. 13–22, 1988.

BERNHARD, J. M.; BARRY, J. P.; BUCK, K. R.; STARCZAK, V. R. Impact of intentionally injected carbon dioxide hydrate on deep-sea benthic foraminiferal survival. **Global Change Biology**, v. 15, n. 8, p. 2078–2088, 2009. Available in: https://doi.org/10.1111/j.1365-2486.2008.01822.x. Access in: 24 oct. 2020.

BERNHARD, J. M.; WIT, J. C.; STARCZAK, V. R.; BEAUDOIN, D. J.; PHALEN, W. G.; MCCORKLE, D. C. Impacts of multiple stressors on a benthic foraminiferal community: a long-term experiment assessing response to ocean acidification, hypoxia and warming. **Frontiers in Marine Science**, v. 8, 2021, p. 1–18. Available in: https://doi.org/10.3389/fmars.2021.643339. Access in: 20 jan. 2022.

CHARRIEAU, L. M.; FILIPSSON, H. L.; NAGAI, Y.; KAWADA, S.; LJUNG, K.; KRITZBERG, E.; TOYOFUKU, T. Decalcification and survival of benthic foraminifera under the combined impacts of varying pH and salinity. **Marine Environmental Research**, v. 138, p. 36–45, 2018. Available in: https://doi.org/10.1016/j.marenvres.2018.03.015. Access in: 8 jan. 2022.

CLARKE, K. R.; GORLEY, R. N. **PRIMER-E. User Manual/Tutorial:** Primer vol. 6. E [*S. l.*]: Ltd., Plymouth, 2006. 182 p.

COTTEY, T. L.; HALLOCK, P. Test surface degradation in *Archaias angulatus*. **Journal of foraminiferal research**, v. 8, n. 3, p. 187–202, 1988. Available in: https://doi.org/10.2113/gsjfr.18.3.187. Access in: 9 jan. 2022.

CROOK, E. D.; COHEN, A. L.; REBOLLEDO-VIEYRA, M.; HERNANDEZ, L.; PAYTAN, A. Reduced calcification and lack of acclimatization by coral colonies growing in areas of persistent natural acidification. **PNAS**, v. 110, n. 27, p. 11044–11049, 2013. Available in: https://doi.org/10.1073/pnas.1301589110. Access in: 15 dec. 2021.

CROOK, E. D.; KROEKER, K. J.; POTTS, D. C.; REBOLLEDO-VIEYRA, M. Recruitment and Succession in a tropical benthic community in response to in-situ ocean acidification. **PLoS ONE**, v. 11, e0146707, 2016. Available in: https://doi.org/10.1371/ journal.pone.0146707. Access in: 15 dec. 2021.

CROOK, E. D.; POTTS, D.; HERNANDEZ, L.; PAYTAN, A. Calcifying coral abundance near low-pH springs: implications for future ocean acidification. **Coral Reefs**, v. 31, p. 239–245, 2012. Available in: https://doi.org/10.1007/s00338-011-0839-y. Access in: 15 dec. 2021.

CULVER, S. J.; BUZAS, M. A. Distribution of recent benthic foraminifera in the Caribbean area. **Smithsonian Contributions to the Marine Sciences,** issue 14, 1982. Available in: https://doi.org/https://doi.org/10.5479/si.01960768.14.1. Access in: 11 feb. 2022.

CUSHMAN, J. A. **The Foraminifera of the Atlantic Ocean**. Netherlands: Smithsonian Institutio, USNM. v. 2, Antiquariat Junk, 1929. 129 p. (Bulletin 104).

DE GOEYSE, S.; WEBB, A. E.; REICHART, G. J.; DE NOOIJER, L. J. Carbonic anhydrase is involved in calcification by the benthic foraminifer *Amphistegina lessonii*. **Biogeosciences**,

v. 18, p. 393–401, 2021. Available in: https://doi.org/10.5194/bg-18-393-2021. Access in: 20 feb. 2022.

DE NOOIJER, L. J.; LANGER, G.; NEHRKE, G.; BIJMA, J. Physiological controls on seawater uptake and calcification in the benthic foraminifer *Ammonia tepida*. **Biogeosciences**, v. 6, p. 2669–2675, 2009. Available in: https://doi.org/10.5194/bg-6-2669-2009. Access in: 22 nov. 2021.

DIAS, B. B.; HART, M. B.; SMART, C. W.; HALL-SPENCER, J. M. Modern seawater acidification: the response of foraminifera to high-CO_2 conditions in the Mediterranean Sea. **Journal of the Geological Society**, v. 167, p. 843–846, 2010. Available in: https://doi.org/10.1144/0016-76492010-050. Access in: 17 jul. 2020.

DICKSON, A. G.; SABINE, C. L.; CHRISTIAN, J. R. **Guide to best practices for ocean CO_2 measurements.** Sidney, BC, Canada: North Pacific Marine Science Organization, 2007.

DONEY, S. C.; BUSCH, D. S.; COOLEY, S. R.; KROEKER, K. J. The Impacts of Ocean Acidification on Marine Ecosystems and Reliant Human Communities. **Annual Reviews**, v. 45, p. 83–112, 2020. Available in: https://doi.org/10.1146/annurev-environ-012320-083019. Access in: 20 feb. 2022.

DONEY, S. C.; FABRY, V. J.; FEELY, R. A.; KLEYPAS, J. A. Ocean acidification: the other CO_2 problem. **Annual Review of Marine Science**, v. 1, p. 169–192, 2009. Available in: https://doi.org/10.1146/annurev.marine.010908.163834. Access in: 22 feb. 2022.

DONG, S.; LEI, Y.; LI, T.; JIAN, Z. Changing structure of benthic foraminiferal communities due to declining pH: Results from laboratory culture experiments. **Science China Earth Science**, v. 62, p. 1151–1166, 2019. Available in: https://doi.org/https://doi.org/10.1007/s11430-018-9321-6. Access in: 29 oct. 2020.

DONG, S.; LEI, Y.; LI, T.; JIAN, Z. Response of benthic foraminifera to pH changes: Community structure and morphological transformation studies from a microcosm experiment. **Marine Micropaleontology**, v. 156, 101819, 2020. Available in: https://doi.org/10.1016/j.marmicro.2019.101819. Access in: 4 jan. 2022.

DOO, S. S.; HAMYLTON, S.; FINFER, J.; BYRNE, M. Spatial and temporal variation in reef-scale carbonate storage of large benthic foraminifera: a case study on One Tree Reef. **Coral Reefs**, v. 36, p. 293–303, 2016. Available in: https://doi.org/10.1007/s00338-016-1506-0. Access in: 12 jul. 2020.

ENGEL, B. E.; HALLOCK, P.; PRICE, R. E.; PICHLER, T. Shell dissolution in larger benthic foraminifers exposed to pH and temperature extremes: Results from an in situ experiment. **Journal of Foraminiferal Research**, v. 45, n. 2, p. 190–203, 2015. Available in: https://doi.org/10.2113/gsjfr.45.2.190. Access in: 6 jan. 2022.

EYRE, B. D.; CYRONAK, T.; DRUPP, P.; DE CARLOS, E. H.; SACH, J. P.; ANDERSSON, A. J. Coral reefs will transition to net dissolving before end of century. **Science**, v. 359, n. 6378, p. 908–911, 2018. Available in://doi.org/10.1126/science.aao1118. Access in: 10 jul. 2020.

FUJITA, K.; HIKAMI, M.; SUZUKI, A.; KUROYANAGI, A.; SAKAI, K.; KAWAHATA, H.; NOJIRI, Y. Effects of ocean acidification on calcification of symbiont-bearing reef foraminifers. **Biogeosciences**, v. 8, p. 2089–2098, 2011. Available in: https://doi.org/10.5194/bg-8-2089-2011. Access in: 17 jul. 2020.

GEERKEN, E.; DE NOOIJER, L. J.; TOYOFUKU, T.; ROEPERT, A.; MIDDELBURG, J. J.; KIENHUIS, M. V. M.; NAGAI, Y.; POLERECKY, L.; REICHART, G. J. High precipitation rates characterize biomineralization in the benthic foraminifer *Ammonia beccarii*. **Geochimica et Cosmochimica Acta**, v. 318, p. 70–82, 2022. Available in: https://doi.org/10.1016/j.gca.2021.11.026. Access in: 5 jan. 2022.

GISCHLER, E.; MÖDER, A. Modern benthic foraminifera on Banco Chinchorro, Quintana Roo, Mexico. **Facies**, v. 55, p. 27–35, 2009. Available in: https://doi.org/10.1007/s10347-008-0162-4. Access in: 12 jul. 2020.

GUAMÁN-GUEVARA, F.; AUSTIN, H.; HICKS, N.; STREETER, R.; AUSTIN, W. E. N. Impacts of ocean acidification on intertidal benthic foraminiferal growth and calcification. **PLoS ONE**, v. 14, n. 8, e0220046, 2019. Available in: https://doi.org/10.1371/journal.pone.0220046. Access in: 12 jul. 2022.

HALLOCK, P.; LIDZ, B. H.; BURKHARD-COCKEY, E. M.; DONNELLY, K. B. Foraminifera as bioindicators in coral reef assessment and monitoring: The FORAM Index. **Environmental Monitoring and Assessment**, v. 81, p. 221–238, 2003. Available in: https://doi.org/10.1023/A:1021337310386. Access in: 24 oct. 2020.

HAYNERT, K.; SCHÖNFELD, J.; POLOVODOVA-ASTEMAN, I.; THOMSEN, J. The benthic foraminiferal community in a naturally CO_2-rich coastal habitat in the southwestern Baltic Sea. **Biogeosciences**, v. 9, p. 4421–4440, 2012. Available in: https://doi.org/10.5194/bgd-9-7783-2012. Access in: 24 oct. 2020.

HUGHES, T. P.; BARNES, M. L.; BELLWOOD, D. R.; CINNER, J. E.; CUMMING, G. S.; JACKSON, J. B.C.; KLEYPAS, J.; VAN DE LEEMPUT, I. A.; LOUGH, J. M.; MORRISON, T. H.; PALUMBI, S. R.; VAN NES, E. H.; SCHEFFER, M. Coral reefs in the Anthropocene. **Nature**, v. 546, p. 82–90, 2017. Available in: https://doi.org/10.1038/nature22901. Access in: 9 jan. 2022.

INTERGOVERNMENTAL PANEL ON CLIMATE CHANGE. **Climate Change 2021:** the physical science basis. Cambridge, U.K.: Cambridge University Press, 2021. In Press.

JONES, R.W. **The Challenger Foraminifera** – The Natural History Museum. London: Oxford University Press, 1994. 149 p.

KAWAHATA, H.; FUJITA, K.; IGUCHI, A.; INOUE, M.; IWASAKI, S.; KUROYANAGI, A.; MAEDA, A.; MANAKA, T.; MORIYA, K.; TAKAGI, H.; TOYOFUKU, T.; YOSHIMURA, T.; SUZUKI, A. Perspective on the response of marine calcifiers to global warming and ocean acidification — Behavior of corals and foraminifera in a high CO_2 world "hot house". **Progress in Earth and Planetary Science**, v. 6, n. 5, p. 1–37, 2019. Available in: https://doi.org/https://doi.org/10.1186/s40645-018-0239-9. Access in: 12 jul. 2020.

KNORR, P. O.; ROBBINS, L. L.; HARRIES, P. J.; HALLOCK, P.; WYNN, J. Response of the miliolid *Archaias angulatus* to simulated ocean acidification. **Journal of Foraminiferal Research**, v. 45, n. 2, p. 109–127, 2015. Available in: https://doi.org/10.2113/gsjfr.45.2.109. Access in: 6 jan. 2022.

KÖHLER-RINK, S.; KÜHL, M. Microsensor studies of photosynthesis and respiration in larger symbiotic foraminifera. I The physico-chemical microenvironment of *Marginopora vertebralis*, *Amphistegina lobifera* and *Amphisorus hemprichii*. **Marine biology** v. 137, p. 473–486, 2000. Available in: https://doi.org/10.1007/s002270000335. Access in: 8 jan. 2022.

KROEKER, K. J.; KORDAS, R. L.; CRIM, R.; HENDRIKS, I. E.; RAMAJO, L.; SINGH, G. S.; DUARTE, C. M.; GATTUSO, J. P. Impacts of ocean acidification on marine organisms: quantifying sensitivities and interaction with warming. **Global Change Biology**, v. 19, p. 1884–1896, 2013. Available in: https://doi.org/10.1111/gcb.12179. Access in: 26 nov. 2020.

KUROYANAGI, A.; IRIEM, T.; KINOSHITA, S.; KAWAHATA, H.; SUZUKI, A.; NISHI, H.; SASAKI, O.; TAKASHIMA, REISHI; FUJITA, K. Decrease in volume and density of foraminiferal shells with progressing ocean acidification. **Scientific reports**, v. 11, 19988, 2021. Available in: https://doi.org/10.1038/s41598-021-99427-1. Access in: 27 nov. 2020.

KWIATKOWSKI, L.; TORRES, O.; BOPP, L.; AUMONT, O.; CHAMBERLAIN, M.; CHRISTIAN, J.; DUNNE, J.; GEHLEN, M.; ILYINA, T.; JOHN, J.; LENTON, A.; LI, H.; LOVENDUSKI, N.; ORR, J.; PALMIERI, J.; SCHWINGER, J.; SÉFÉRIAN, R.; STOCK, C.; TAGLIABUE, A.; ZIEHN, T. Twenty-first century ocean warming, acidification, deoxygenation, and upper ocean nutrient decline from CMIP6 model projections. **Biogeosciences**, v. 17, p. 3439–3470, 2020. Available in: https://doi.org/10.5194/bg-2020-16. Access in: 1 oct. 2022.

LANGER, M. R. Assessing the contribution of foraminiferan protists to global ocean carbonate production. **Journal of Eukaryotic Microbiology**, v. 55, n. 3, p. 163–169, 2008. Available in: https://doi.org/10.1111/j.1550-7408.2008.00321.x. Access in: 12 jul. 2020.

LANGER, M. R.; LIPPS, J. H.; SILK, M. T.; LIPPS, J. H. Global ocean carbonate and carbon dioxide production: the role of reef foraminifera. **Journal of Foraminiferal Research**, v. 27, n. 4, p. 271–277, 1997. Available in: https://doi.org/10.2113/gsjfr.27.4.271. Access in: 12 jul. 2020.

LE QUÉRÉ, C.; ANDREW, R. M.; FRIEDLINGSTEIN, P.; SITCH, S.; HAUCK, J.; PONGRATZ, J.; PICKERS, P. A.; KORSBAKKEN, J. I.; PETERS, G. P.; CANADELL, J. G.; ARNETH, A.; ARORA, V. K.; BARBERO, L.; BASTOS, A.; BOPP, L.; CHEVALLIER, F.; CHINI, L. P.; CIAIS, P.; DONEY, S. C.; ZHENG, B. Global Carbon Budget 2018. **Earth System Science Data**, v. 10, n. 4, p. 2141–2194, 2018. Available in: https://doi.org/10.5194/essd-10-2141-2018. Access in: 25 jan. 2022.

LICKER, R.; EKWURZEL, B.; DONEY, S. C.; COOLEY, S. R.; LIMA, I. D.; HEEDE, R.; FRUMHOFF, P. C. Attributing ocean acidification to major carbon producers. **Environmental Research Letters**, v. 14, n. 12, 124060, 2019. Available in: https://doi.org/10.1088/1748-9326/ab5abc. Access in: 8 jan. 2022.

LIDA, Y.; TAKATANI, Y.; KOJIMA, A.; ISHII, M. Global trends of ocean CO_2 sink and ocean acidification: an observation-based reconstruction of surface ocean inorganic carbon variables. **Journal of Oceanography**, v. 77, 323–358, 2020. Available in: https://doi.org/10.1007/s10872-020-00571-5. Access in: 10 jan. 2022

LUEKER, T. J.; DICKSON, A. G.; KEELING, C. D. Ocean pCO_2 calculated from dissolved inorganic carbon, alkalinity, and equations for K1 and K2: validation based on laboratory measurements of CO_2 in gas and seawater at equilibrium. **Marine Chemistry**, v. 70, p. 105–119, 2000. Available in: https://doi.org/10.1016/S0304-4203(00)00022-0. Access in: 10 oct. 2021.

LÜTHI, D.; LE FLOCH, M.; BEREITER, B.; BLUNIER, T.; BARNOLA, J. M.; SIEGENTHALER, U.; RAYNAUD, D.; JOUZEL, J.; FISCHER, H.; KAWAMURA, K.; STOCKER, T. F. High-resolution carbon dioxide concentration record 650,000-800,000 years before present**. Nature**, v. 453, p. 379–382, 2008. Available in: https://doi.org/10.1038/nature06949. Access in: 23 jan. 2022.

MARTIN, R. E. Habitat and distribution of the foraminifer *Archaias angulatus* (Fichtel and Moll) (Miliolina, Soritidae), northern Florida Keys. **Journal of Foraminiferal Research**, v. 16, n. 3, p. 201–206, 1986. Available in: https://doi.org/10.2113/gsjfr.16.3.201. Access in: 23 dec. 2021.

MARTINEZ, A.; CROOK, E. D.; BARSHIS, D. J.; POTTS, D. C.; REBOLLEDO-VIEYRA, M.; HERNANDEZ, L.; PAYTAN, A. Species-specific calcification response of Caribbean corals after 2-year transplantation to a low aragonite saturation submarine spring. **Proceedings B**, v. 286, n. 20190572, 2019. Available in: https://dx.doi.org/10.6084/m9. Access in: 12 jul. 2021.

MARTINEZ, A.; HERNÁNDEZ-TERRONES, L.; REBOLLEDO-VIEYRA, M.; PAYTAN, A. Impact of carbonate saturation on large Caribbean benthic foraminifera assemblages. **Biogeosciences**, v. 15, p. 6819–6832, 2018. Available in: https://doi.org/10.5194/bg-15-6819-2018. Access in: 12 jul. 2020.

MILKER, Y.; SCHMIEDL, G. A taxonomic guide to modern benthic shelf foraminifera of the western Mediterranean Sea. **Palaeontologia Electronica**, v. 15, n.2, p. 1–134, 2012. Available in: https://doi.org/10.26879/271. Access in: 15 jul. 2020.

MOODLEY, L.; BOSCHKER, H. T. S.; MIDDELBURG, J. J.; PEL, R.; HERMAN, P. M. J.; DE DECKERE, E.; HEIP, C. H. R. Ecological significance of benthic foraminifera: 13C Labelling experiments. **Marine Ecology Progress Series**, v. 202, p. 289–295, 2000. Available in: https://doi.org/10.3354/meps202289. Access in: 23 jan. 2022.

MURRAY, J. W. **Ecology and applications of Benthic Foraminifera**. Cambridge: Cambridge University Press, 2006. 426 p.

NARAYAN, G. R.; REYMOND, C. E.; STUHR, M.; DOO, S.; SCHMIDT, C.; MANN, T.; WESTPHAL, H. Response of large benthic foraminifera to climate and local changes: Implications for future carbonate production. **Sedimentology**, v. 69, p. 121–161, 2021. Available in: https://doi.org/10.1111/sed.12858. Access in: 23 jan. 2022.

NEHRKE, G.; KEUL, N.; LANGER, G.; DE NOOIJER, L. J.; BIJMA, J.; MEIBOM, A. A new model for biomineralization and trace-element signatures of Foraminifera tests. **Biogeosciences**, v. 10, p. 6759–6767, 2013. Available in: https://doi.org/10.5194/bg-10-6759-2013. Access in: 23 jan. 2022.

NULL, K. A.; KNEE, K. L.; CROOK, E. D.; SIEYES, N. R.; REBOLLEDO-VIEYRA, M.; HERNÁNDEZ-TERRONES, L.; PAYTAN, A. Composition and fluxes of submarine groundwater along the Caribbean coast of the Yucatan Peninsula. **Continental Shelf Research**, v. 77, p. 38–50, 2014. Available in: https://doi.org/10.1016/j.csr.2014.01.011. Access in: 12 jul. 2020.

PENÃ, V.; HARVEY, B. P.; AGOSTINI, S.; PORZIO, L.; MILAZZO, M.; HORTA, P.; GALL, L. L.; HALL-SPENCER, J. M. Major loss of coralline algal diversity in response to ocean acidification. **Global Change Biology,** v. 27, n. 19, p. 4785–4798, 2021. Available in: https://doi.org/10.1111/gcb.15757. Access in: 18 jul. 2021.

PERRY, E.; VELAZQUEZ-OLIMAN, G.; MARIN, L. The hydrogeochemistry of the karst aquifer system of the northern Yucatan peninsula, Mexico. **International Geology Review**, v. 44, p. 191–221, 2002. Available in: https://doi.org/10.2747/0020-6814.44.3.191. Access in: 23 jan. 2022.

PETERS, G. P.; ANDREW, R. M.; CANADELL, J. G.; FRIEDLINGSTEIN, P.; JACKSON, R. B.; KORSBAKKEN, J. I.; LE QUÉRÉ, C.; PEREGON, A. Carbon dioxide emissions continue to grow amidst slowly emerging climate policies. **Nature Climate Change**, v. 10, p. 3–6, 2020. Available in: https://doi.org/10.1038/s41558-019-0659-6. Access in: 26 nov. 2020.

PETTIT, L. R.; HART, M. B.; MEDINA-SÁNCHEZ, A. N.; SMART, C. W.; RODOLFO-METALPA, R.; HALL-SPENCER, J. M.; PROL-LEDESMA, R. M. Benthic foraminifera show some resilience to ocean acidification in the northern Gulf of California, Mexico. **Marine Pollution Bulletin**, v. 73, n. 2, p. 452–462, 2013. Available in: https://doi.org/10.1016/j.marpolbul.2013.02.011. Access in: 20 oct. 2020.

PETIT, J. R.; JOUZEL, J.; RAYNAUD, D.; BARNOLA, J. M.; BASILE, I.; BENDER, M.; CHAPPELLAZ, J.; DAVIS, M.; DELAYGUE, G.; DELMOTTE, M.; KOTLYAKOV, V. M.; LEGRAND, M.; LIPENKOV, V. Y.; LORIUS, C.; PÉPIN, L.; RITZ, C.; SALTZMAN, E.; STIEVENARD, M. Climate and atmospheric history of the past 420,000 years from the Vostok ice core, Antarctica. **Nature**, v. 399, p. 429–436, 1999. Available in: https://doi.org/10.1038/20859. Access in: 26 nov. 2020.

PETTIT, L. R., SMART, C. W., HART, M. B., MILAZZO, M., & HALL-SPENCER, J. M. Seaweed fails to prevent ocean acidification impact on foraminifera along a shallow-water CO_2 gradient. **Ecology and Evolution**, v. 5, n. 9, p. 1–10, 2015. Available in: https://doi.org/10.1002/ece3.1475. Access in: 4 jan. 2022.

PIERROT, D. E.; LEVIS, E.; WALLACE, D. W. R. **MS Excel Program Developedfor CO2 System Calculations.** Oak Ridge, TN: U.S. Department of Energy: Carbon Dioxide Information Analysis Center, Oak Ridge National Laboratory, 2006.

PRAZERES, M., UTHICKE, S., & PANDOLFI, J. M. Ocean acidification induces biochemical and morphological changes in the calcification process of large benthic

foraminifera. **Proceedings B**, v. 282, 20142782, 2015. Available in: https://doi.org/10.1098/rspb.2014.2782. Access in: 12 jul. 2020.

PRICE, N. N.; MARTZ, T. R.; BRAINARD, R. E.; SMITH, J. E. Diel variability in seawater pH relates to calcification and benthic community structure on coral reefs. **PLoS ONE**, v. 7, n. 8, e43843, 2012. Available in: https://doi.org/10.1371/journal.pone.0043843. Access in: 23 jan. 2022.

R CORE TEAM. **R:** a language and environment for statistical computing. [*S. l.: s. n.*], 2020.

RIAHI, K.; VAN VUUREN, D. P.; KRIEGLER, E.; EDMONDS, J.; O'NEILL, B. C.; FUJIMORI, S.; BAUER, N.; CALVIN, K.; DELLINK, R.; FRICKO, O.; LUTZ, W.; POPP, A.; CUARESMA, J. C.; SAMIR, K. C.; LEIMBACK, M.; JIANG, L.; KRAM, T.; RAO, S.; EMMERLING, J.; EBI, K.; HASEGAWA, T.; HAVLIK, P.; HUMPENODER, F.; DA SILVA, L. A.; SMITH, S.; STEHFEST, E.; BOSETTI, V.; EOM, J.; GERNAAT, D.; MASUI,T.; ROGELJ, J.; STREFLER, J.; DROUET, L.; KREY, V.; LUDERER, G.; HARMSEN, M.; TAKAHASHI, K.; BAUMSTARK, L.; DOELMAN, J. C.; KAINUMA, M.; KLIMONT, Z.; MARANGONI, G.; LOTZE-CAMPEN, H.; OBERSTEINER, M.; TABEAU, A.; TAVONI, M. The shared socioeconomic pathways and their energy, land use, and greenhouse gas emissions implications: an overview. **Global Environmental Change**, v. 42, p. 153–168, 2017. Available in: https://doi.org/10.1016/j.gloenvcha.2016.05.009. Access in:

SABINE, C. L.; FEELY, R. A.; GRUBER, N.; KEY, R. M.; LEE, K.; BULLISTER, J. L.; WANNINKHOF, R.; WONG, C. S.; WALLACE, D.W. R.; TILBROOK, B.; MILLERO, F. J.; PENG, T. H.; KOZYR, A.; ONO, T.; RIOS, A. F. The oceanic sink for anthropogenic CO_2. **Science**, v. 305, p. 367–371, 2004. Available in: https://doi.org/10.1126/science.1097403. Access in: 20 jan. 2022.

SARIASLAN, N.; LANGER, M. R. Atypical, high-diversity assemblages of foraminifera in a mangrove estuary from Northern Brazil. **Biogeosciences**, v. 18, p. 4073–4090, 2021. Available in: https://doi.org/https://doi.org/10.5194/bg-2021-56. Access in: 25 jul. 2021.

SCHIEBEL, R. Planktic foraminiferal sedimentation and the marine calcite budget. **Global Biochemical Cycles**, v. 16, n. 4, p. 3-1–3-21, 2002. Available in: https://doi.org/10.1029/2001GB001459. Access in: 21 sep. 2020.

SCHNEIDER, C. A.; RASBAND, W. S.; ELICEIRI, K. W. NIH Image to ImageJ: 25 years of image analysis. **Nature Methods**, v. 9, n. 7, p. 671–675, 2012. Available in: https://doi.org/10.1038/nmeth.2089. Access in: 23 jan. 2022.

SINUTOK, S.; HILL, R.; KUHL, M.; DOBLIN, M. A.; RALPH, P. J. Ocean acidification and warming alter photosynthesis and calcification of the symbiont-bearing foraminifera *Marginopora vertebralis*. **Marine Biology**, v. 161, p. 2143–2154, 2014. Available in: https://doi.org/10.1007/s00227-014-2494-7. Access in: 18 oct. 2020.

STEPHENSON, C. M.; HALLOCK, P.; KELMO, F. Foraminiferal assemblage indices: A comparison of sediment and reef rubble samples from Conch Reef, Florida, USA. **Ecological Indicators**, v. 48, p. 1–7, 2015. Available in: https://doi.org/10.1016/j.ecolind.2014.07.004. Access in: 9 dec. 2021.

STUHR, M.; CAMERON, L. P.; BLANK-LANDESHAMMER, B.; REYMOND, C. E.; DOO, S. S.; WESTPHAL, H.; SICKMANN, A.; RIES, J. B. Divergent proteomic responses offer insights into resistant physiological responses of a reef-foraminifera to climate change scenarios. **Oceans**, v. 2, p. 281–314, 2021. Available in: https://doi.org/10.3390/oceans2020017. Access in: 6 jan. 2022.

TOYOFUKU, T.; MATSUO, M. Y.; DE NOOIJER, L. J.; NAGAI, Y.; KAWADA, S.; FUJITA, K.; REICHART, G. J.; NOMAKI, H.; TSUCHIYA, M.; SAKAGUCHI, H.; KITAZATO, H. Proton pumping accompanies calcification in foraminifera. **Nature Communications**, v. 8, n. 1, 14145, 2017. Available in: https://doi.org/10.1038/ncomms14145. Access in: 22 nov. 2021.

UPPSTRÖM, L. R. The boron/chlorinity ratio of deep-sea water from the Pacific Ocean. **Deep Sea Research and Oceanographic Abstracts**, v. 21, p. 161–162, 1974.

UTHICKE, S.; MOMIGLIANO, P.; FABRICIUS, K. E. High risk of extinction of benthic foraminifera in this century due to ocean acidification. **Scientific Reports**, v. 3, n. 1769, p. 1–5, 2013. Available in: https://doi.org/10.1038/srep01769. Access in: 18 oct. 2020.

WEINMANN, A. E.; LANGER, M. R.; GOLDSTEIN, S. T.; TRIANTAPHYLLOU, M. V. Community responses of intertidal foraminifera to pH variations: a culture experiment with propagules. **Aquatic Ecology**, v. 55, p. 309–325, 2021. Available in: https://doi.org/10.1007/s10452-021-09833-w. Access in: 4 jan. 2022.

WILSON B.; WILSON, J.I. Shoreline foraminiferal thanatacoenoses around five eastern Caribbean islands and their environmental and biogeographic implications. **Continental Shelf Research**, v. 31, n. 7–8, p. 857–866, 2011. Available in: https://doi.org/10.1016/j.csr.2011.02.010. Access in: 10 jan. 2022.

YAMANO, H.; MIYAJIMA, T.; KOIKE, I. Importance of foraminifera for the formation and maintenance of a coral sand cay: Green Island, Australia. **Coral Reefs**, v. 19, p. 51–58, 2000. Available in: https://doi.org/10.1007/s003380050226. Access in: 23 jan. 2022.

APPENDIX

APPENDIX A – ALPHABETICAL LIST OF ORDER, FAMILY, GENUS AND SPECIES FOUND AT PUERTO MORELOS REEF LAGOON SPRINGS, QR MEXICO

Order	Family	Genus	Species
Miliolida	Alveolinidae	Borelis	*Borelis pulchra* (d'Orbigny, 1839)
	Cornuspiridae	Cornuspira	*Cornuspira involvens* (Reuss, 1850)
	Fischerinidae	Trisegmentina	*Trisegmentina compressa* Wiesner, 1923
	Hauerinidae	Affinetrina	*Affinetrina* conf. *Affinetrina planciana* (d'Orbigny, 1839)
			Affinetrina quadrilateralis (d'Orbigny, 1839)
			Affinetrina sp
		Agglutinella	*Agglutinella compressa* El-Nakhal, 1983
		Articulina	*Articulina pacifica* Cushman, 1944
			Articulina sp
			Articulina sulcata (Reuss, 1850)
		Cycloforina	*Cycloforina contorta* (d'Orbigny, 1846)
		Hauerina	*Hauerina ornatissima* (Karrer, 1868)
		Lachlanella	*Lachlanella carinata* (d'Orbigny, 1839)
		Miliolinela	*Miliolinela* sp.13
			Miliolinella circularis (Bornemann, 1855)
			Miliolinella elongata Kruit, 1955
			Miliolinella sp.11
			Miliolinella sp.a
			Miliolinella subrotunda (Montagu, 1803)
			Miliolinella webbiana (d'Orbigny, 1839)
		Pseudolachlanella	*Pseudolachlanella eburnea* (d'Orbigny, 1839)
			Pseudolachlanella slitella Langer, 1992
		Pseudotriloculina	*Pseudotriloculina limbata* (d'Orbigny in Fornasini, 1905)
			Pseudotriloculina linneiana (d'Orbigny, 1839)
			Pseudotriloculina sp.
			Pseudotriloculina tricarinata triangular
		Pyrgo	*Pyrgo* conf. *Pyrgo elongata*
			Pyrgo sp.1
		Quinqueloculina	*Quinqueloculina bosciana* d'Orbigny, 1839
			Quinqueloculina carinatastriata (Wiesner, 1923)
			Quinqueloculina cf. *berthelotiana*
			Quinqueloculina cf. *zengui*

			Quinqueloculina conf. *Quinqueloculina bradyana*
			Quinqueloculina conf. *Quinqueloculina distorqueata*
			Quinqueloculina disparilis d'Orbigny, *1826*
			Quinqueloculina jugosa (Cushman, 1944)
			Quinqueloculina laevigata (d'Orbigny, 1839)
			Quinqueloculina parkeri (Brady, 1881)
			Quinqueloculina polygona d'Orbigny, 1839
			Quinqueloculina seminulum (Linnaeus, 1758)
			Quinqueloculina sp.12
			Quinqueloculina sp.13
			Quinqueloculina sp.22
			Quinqueloculina sp.22
			Quinqueloculina sp.28
			Quinqueloculina sp.7
			Quinqueloculina subpoeyana Cushman, 1922
			Quinqueloculina tricarinata d'Orbigny, 1839
			Quinqueloculina tropicalis Cushman, 1924
			Quinqueloculina cuvieriana (d'Orbigny, 1826)
		Schlumbergerina	*Schlumbergerina alveoliniformis (Brady, 1879)*
		Siphonaperta	*Siphonaperta agglutinans* (d'Orbigny)
			Siphonaperta distorqueata (Cushman)
			Siphonaperta macbeathi Vella, 1957
		Spirosigmoilina	*Spirosigmoilina* sp
		Triloculina	*Triloculina bertheliniana* (Brady, 1884)
			Triloculina oblonga (Montagu, 1803)
			Triloculina sp
			Triloculina sp.1
			Triloculina tricarinata (d'Orbigny in Deshayes, 1832)
			Triloculina trigonula (Lamarck, 1804)
		Varidentella	*Varidentella* cf. *neostriatula* (Thalmann, 1950)
			Varidentella sp
		Sigmoihauerina	*Sigmoihauerina involuta* (Cushman, 1946)
		Sigmoilinita	*Sigmoilinita* conf. *Sigmoilinita costata Schlumberger*
	Peneroplidae	Euthymonacha	*Euthymonacha polita* (Chapman, 1900)
		Laevipeneroplis	*Laevipeneroplis proteus* (d'Orbigny, 1839)
		Peneroplis	*Peneroplis (Peneroplis)*

			carinatus d'Orbigny, 1839
			Peneroplis pertustus (Forskal, 1775)
			Peneroplis planatus (Fichtel & Moll, 1798)
		Spirolina	*Spirolina acicularis* (Barst, 1791)
	Riveroinidae	Pseudohauerina	*Pseudohauerina diversa* (Cushman, 1946)
		Pseudohauerinella	*Pseudohauerinella* conf. *Pseudohauerinella dissidens*
	Soritidae	Archaias	*Archaias angulatus* (Fichtel & Moll, 1798)
		Cyclorbiculina	*Cyclorbiculina compressa* (d'Orbigny, 1839)
		Parasorites	*Parasorites orbitolitoides* (Hofker, 1930)
		Sorites	*Sorites marginalis* (Lamarck, 1816)
	Spiroloculinidae	Spiroloculina	*Spiroloculina acescata* (Cushman, 1932)
			Spiroloculina antillarum d'Orbigny, 1839
			Spiroloculina corrugata Cushman & Todd, 1944
			Unidentified calcareous foraminifera 1
			Unidentified calcareous foraminifera 2
			Unidentified calcareous foraminifera 4
			Unidentified calcareous foraminifera
			Unidentified calcareous foraminifera 6
Polymorphinida	Ellipsolagenidae	Fissurina	*Fissurina* sp
Rotaliida	Amphisteginidae	Amphistegina	*Amphistegina gibbosa* d'Orbigny, 1839
	Acervulinidae	Planogypsina	*Planogypsina acervalis* (Brady, 1884)
		acervulina	*Acervulina inhaerens* Schultze, 1854
	Asterigerinidae	Asterigerina	*Asterigerina carinata* d'Orbigny, 1839
	Bolivinitidae	Bolivina	*Bolivina densipunctata* Sellier de Civrieux, 1976
		Sigmavirgulina	*Sigmavirgulina tortuosa* (Brady, 1881)
	Buliminidae	Bulimina	*Bulimina* sp
	Cancrisidae	Cancris	*Cancris* sp
	Cibicididae	Cibicides	*Cibicides lobatulus* (Walker & Jacob, 1798)
		Cibicidoides	*Cibicidoides mundulus* (Brady, Parker & Jones, 1888)
			Cibicidoides sp
	Cymbaloporidae	Cymbaloporetta	*Cymbaloporetta* sp
			Cymbaloporetta squammosa (d'Orbigny, 1839)
		Millettiana	*Millettiana sp*
	Discorbidae	Rotorbis	*Rotorbis auberii* (d'Orbigny, 18239)
		Strebloides	*Strebloides advena* (Cushman, 1922)
		Trochulina	*Trochulina* sp
	Elphidiidae	Cribroelphidium	*Cribroelphidium bartletti* (Cushman, 1933)
			Cribroelphidium excavatum (Terquem,

			1875)
		Elphidium	*Elphidium conf Elphidium williamsome ou fijense*
			Elphidium discoidale (d'Orbigny, 1839)
			Elphidium excavatum
	Globigerinidae	Globigerinella	*Globigerinella calida* (Parker, 1962)
		Globigerinoides	*Globigerinoides ruber* (d'Orbigny, 1839)
	Homotrematidae	Miniacina	*Miniacina miniacea* (Pallas, 1766)
	Melonidae	Melonis	*Melonis* ?
	Nonionidae	Nonionella	*Nonionella* sp
		Nonionoides	*Nonionoides grateloupi* (d'Orbigny, 1839)
	Nummulitidae	Heterostegina	*Heterostegina depressa* d'Orbigny, 1826
	Planorbulinidae	Caribeanella	*Caribeanella* conf. *polystoma* (Bermúdez, 1952)
		Planorbulina	*Planorbulina mediterranensis* d'Orbigny, 1826
	Reussellidae	Reussella	*Reussella atlantica* Cushman, 1947
	Rosalinidae	Neoconorbina	*Neoconorbina terquemi* (Rzehak, 1888)
		Rosalina	*Rosalina* cf. *floridana* (Cushman, 1922)
			Rosalina globularis d'Orbigny, 1826
			Rosalina sp
		Tretomphalus	*Tretomphalus bulloides (d'Orbigny, 1839)*
	Rotaliidae	Rotorbinella	*Rotorbinella rosea* (d'Orbigny in Guérin-Méneville, 1832)
	Siphogenerinoididae	Siphogenerina	*Siphogenerina raphana* (Parker & Jones, 1865)
	Siphoninidae	Siphonina	*Siphonina bradyana* Cushman, 1927
			Siphonina reticulata (Čžjžek, 1848)
	Turrilinidae	Floresina	*Floresina* sp
	Uvigerinidae	Angulogerina	*Angulogerina* sp
			Unidentified calcareous foraminifera 3
			Unidentified calcareous foraminifera 5
Spirillinida	Planispirillinidae	Planispirillina	*Planispirillina inaequalis* (Brady, 1879)
Textulariida	Reophacidae	Reophax	*Reophax* sp.1
			Reophax sp.2
	Textulariidae	Textularia	*Textularia agglutinans* (d'Orbigny, 1839)
			Textularia sp.1
	Valvulinidae	Clavulina	*Clavulina angularis* d'Orbigny, 1826
		Valvulina	*Valvulina oviedoiana* (d'Orbigny, 1839a)
			Unidentified agglutinated foraminifera 1
			Unidentified agglutinated foraminifera 2
			Unidentified agglutinated foraminifera 3

APPENDIX B – RAW DATA OF FUNCTIOAL AND TEST TYPE GROUPS

Sample ID	Agglutinated (%)	Opportunistic (%)	Small miliolids (%)	Small rotaliids (%)	Symbiont bearing (%)
1	9.1	0.0	27.8	37.5	25.6
2	16.4	0.0	45.3	18.8	19.5
3	11.6	0.0	47.3	21.4	19.6
4	15.2	0.0	31.9	35.1	17.8
5	13.2	0.5	22.1	45.8	18.4
6	19.5	0.0	18.4	11.4	50.8
7	9.8	0.6	20.2	23.1	46.2
8	10.7	0.4	22.2	20.4	46.2
9	7.6	0.7	22.9	28.4	40.4
10	6.3	0.7	20.1	25.0	47.8
11	5.9	1.7	27.7	29.8	34.9
12	7.3	2.2	37.7	20.5	31.9
13	4.0	2.4	37.3	26.5	29.7
14	2.3	1.2	46.7	26.5	23.3
15	2.2	4.0	42.0	27.6	24.2
16	9.1	0.0	31.0	34.5	25.4
17	11.0	1.9	41.6	24.0	21.4
18	8.3	0.5	37.6	28.8	24.9
19	8.4	1.9	30.4	34.6	24.3
20	5.1	2.6	38.7	20.9	32.3
21	1.5	0.4	22.7	61.7	13.6
22	1.3	0.4	35.0	50.9	12.4
23	1.6	0.0	40.5	42.1	15.9
24	1.2	1.2	58.5	28.9	10.3
25	0.0	1.4	39.5	44.9	14.1
43	11.5	1.0	20.6	41.5	25.4
44	9.5	1.3	33.2	32.8	23.3
45	10.5	3.5	36.8	31.4	17.8
46	6.5	1.6	34.5	38.3	18.9

APPENDIX C – SIMPER RESULTS

Assemblage	Av. similarity:	Species	Av.Abund	Av.Sim	Contrib%	Cum.%
a	82.14	*Archaias angulatus*	6.8	24.7	30	30
		Quinqueloculina tricarinata	3.6	12.3	15	45
		Rotorbinella rosea	3.6	10.7	13	58
		Cyclorbiculina compressa	2.7	9.5	12	70
		Amphistegina lessonii	2.7	8.6	10	80
		Valvulina oviedoiana	2.3	7.8	9	90
		Quinqueloculina disparilis	1.6	4.8	6	95
b	75.36	*Archaias angulatus*	4.4	16.5	22	22
		Amphistegina lessonii	3.4	14.5	19	41
		Rotorbinella rosea	1.5	6.8	9	50
		Valvulina oviedoiana	1.9	6.6	9	59
		Cyclorbiculina compressa	1.3	6.1	8	67
		Quinqueloculina disparilis	1.2	5.6	7	74
		Agglutinella compressa	1.2	5.3	7	81
		Planorbulina mediterranensis	0.9	3.4	5	86
		Asterigerina carinata	0.8	3.1	4	90
g	70.7	*Archaias angulatus*	7.1	8.9	13	13
		Rotorbinella rosea	6.2	6.7	9	22
		Asterigerina carinata	5.6	5.8	8	30
		Quinqueloculina disparilis	4.7	5.4	8	38
		Amphistegina lessonii	5.4	5.3	7	45
		Rotorbis auberii	4.9	4.9	7	52
		Laevipeneroplis proteus	3.2	3.4	5	57
		Clavulina angularis	2.8	3.2	4	62
		Peneroplis pertustus	2.7	2.7	4	65
		Textularia agglutinans	2.7	2.7	4	69
		Agglutinella compressa	2.5	2.3	3	72
		Valvulina oviedoiana	2.2	2.3	3	76

		Cyclorbiculina compressa	2.3	2.1	3	79
		Rosalina cf. *floridana*	1.9	1.8	3	81
		Lachlanella carinata	1.6	1.4	2	83
		Sorites marginalis	1.8	1.3	2	85
		Quinqueloculina bosciana	2.0	1.1	2	87
		Quinqueloculina subpoeyana	1.9	1.1	2	88
		Articulina pacifica	1.6	1.1	1	90
		Schlumbergerina alveoliniformis	1.6	1.0	1	91
f	74.03	*Rotorbinella rosea*	11.4	7.1	10	10
		Asterigerina carinata	9.9	6.6	9	18
		Archaias angulatus	8.8	5.5	7	26
		Rotorbis auberii	8.0	5.5	7	33
		Laevipeneroplis proteus	7.5	4.8	6	40
		Quinqueloculina disparilis	7.4	4.2	6	45
		Rosalina cf. *floridana*	6.7	4.2	6	51
		Quinqueloculina bosciana	6.0	4.0	5	57
		Peneroplis pertustus	6.1	3.9	5	62
		Textularia agglutinans	5.4	3.7	5	67
		Articulina pacifica	5.2	3.6	5	72
		Quinqueloculina subpoeyana	6.0	3.6	5	76
		Amphistegina lessonii	4.8	3.2	4	81
		Clavulina angularis	5.3	2.4	3	84
		Miliolinella elongata	6.2	2.4	3	87
		Sorites marginalis	3.7	2.4	3	91
e	84.93	*Asterigerina carinata*	12.0	6.7	8	8
		Trochulina sp	10.3	5.8	7	15
		Sorites marginalis	8.8	5.0	6	21
		Laevipeneroplis proteus	8.9	4.9	6	26
		Rosalina cf. *R. floridana*	8.3	4.6	5	32
		Rotorbis auberii	9.2	4.4	5	37
		Quinqueloculina	9.0	4.3	5	42

		subpoeyana				
		Peneroplis pertustus	7.0	3.9	5	46
		Planogypsina acervalis	8.6	3.9	5	51
		Quinqueloculina bosciana	7.4	3.9	5	56
		Agglutinella compressa	6.5	3.5	4	60
		Articulina pacifica	7.2	3.5	4	64
		Peneroplis planatus	7.4	3.5	4	68
		Rotorbinella rosea	6.2	3.5	4	72
		Archaias angulatus	6.4	3.3	4	76
		Rosalina globularis	5.5	3.1	4	80
		Quinqueloculina conf. *Q.distorqueata*	5.0	2.6	3	83
		Textularia agglutinans	5.4	2.6	3	86
		Affinetrina quadrilateralis	4.6	2.4	3	89
		Cibicidoides sp	4.8	2.4	3	92
c	66.01	*Archaias angulatus*	5.3	14.3	22	22
		Amphistegina lessonii	2.2	5.9	9	31
		Valvulina oviedoiana	1.8	5.5	8	39
		Asterigerina carinata	2.0	5.4	8	47
		Rotorbinella rosea	2.5	4.9	7	55
		Quinqueloculina disparilis	2.1	4.4	7	61
		Rotorbis auberii	1.3	3.9	6	67
		Cyclorbiculina compressa	0.9	2.7	4	71
		Rosalina globularis	1.0	2.6	4	75
		Clavulina angularis	0.9	2.3	4	79
		Rosalina cf. R. floridana	0.9	2.0	3	82
		Articulina pacifica	0.7	2.0	3	85
		Quinqueloculina conf. *Q. distorqueata*	1.1	1.9	3	88
		Lachlanella carinata	0.9	1.7	3	90
d	70.26	*Rotorbinella rosea*	7.6	11.4	16	16
		Archaias angulatus	4.6	6.9	10	26
		Cibicidoides sp	3.0	4.3	6	32
		Sorites marginalis	2.6	3.9	6	38

Affinetrina quadrilateralis	2.6	3.9	6	43
Quinqueloculina cf. *berthelotiana*	2.6	3.7	5	48
Quinqueloculina carinatastriata	3.0	3.7	5	54
Laevipeneroplis proteus	2.3	3.2	5	58
Peneroplis pertustus	2.4	3.2	5	63
Miliolinella elongata	2.0	3.2	4	67
Quinqueloculina bosciana	2.4	3.1	4	72
Trochulina sp	2.3	2.9	4	76
Lachlanella carinata	1.7	2.6	4	80
Pseudotriloculina linneiana	1.8	2.5	4	83
Asterigerina carinata	1.7	2.5	4	87
Spiroloculina corrugata	1.6	1.7	2	89
Textularia agglutinans	0.9	1.1	2	91

APPENDIX D – RAW DATA OF TAPHONOMICAL, ASSEMBLAGE TEST SIZE AND TAXONOMIC METRICS

Sample ID	Dissolved %	Broken %	S	N	J'	H'(loge)	Size
1	80	70	19	114	0.62	1.8	0.83
2	80	64	14	103	0.62	1.6	0.98
3	85	80	11	80	0.66	1.6	0.99
4	79	75	21	114	0.66	2.0	0.84
6	78	36	21	63	0.58	1.8	0.91
7	77	47	32	36	0.67	2.3	0.94
8	69	37	31	220	0.71	2.4	0.52
9	62	35	44	480	0.79	3.0	0.30
10	68	41	40	396	0.73	2.7	0.31
12	64	38	55	568	0.87	3.5	0.20
13	61	34	52	1092	0.86	3.4	0.15
14	53	29	68	1882	0.91	3.8	0.14
15	52	27	71	2167	0.91	3.9	0.15
16	78	36	29	112	0.67	2.3	0.59
17	71	43	35	68	0.66	2.3	0.76
18	68	43	52	56	0.79	3.1	0.55
19	69	40	47	307	0.80	3.1	0.31
20	61	33	58	460	0.84	3.4	0.25
21	75	54	42	211	0.65	2.4	0.24
22	68	57	32	139	0.72	2.5	0.30
23	68	43	37	138	0.80	2.9	0.21
24	53	28	44	189	0.85	3.2	0.13
25	68	47	42	400	0.80	3.0	0.17
44	63	43	53	225	0.81	3.2	0.50
45	46	32	57	1392	0.89	3.6	0.16
46	51	28	65	471	0.81	3.4	0.32

APPENDIX E – RAW DATA OF TEST DENSITY, CHAMBER WALL THICKNESS, TEST VOLUME, AND TEST DIAMETER MEASURED IN *ARCHAIAS ANGULATUS* INDIVIDUALS LIVING AT LOW (7.1 PH UNITS) AND HIGH-PH CONDITIONS (8.1 PH UNITS) AT SPRING GORGOS

Individual ID	pH	Density g/cm³	Chamber wall thickness mm³	Volume mm³	Test diameter mm
1	7.96	2.17	0.048	0.10521	0.826
2	7.96	2.79	0.037	0.05552	0.750
3	7.96	2.29	0.041	0.03342	0.794
4	7.96	2.49	0.053	0.03757	0.819
5	7.11	1.28	0.044	0.04886	0.819
6	7.11	1.34	0.054	0.04612	0.851
7	7.11	1.35	0.051	0.03704	0.693
8	7.11	1.32	0.055	0.06280	0.737